

**NISTIR 4496**

**NEW NIST PUBLICATION**

April/May 1991

**Center for Electronics and  
Electrical Engineering**

# **Technical Progress Bulletin**

Covering Center Programs,  
July to September 1990,  
with 1991 CEEE Events Calendar

**U.S. DEPARTMENT OF COMMERCE  
National Institute of Standards  
and Technology  
Center for Electronics and  
Electrical Engineering  
Semiconductor Electronics Division  
Gaithersburg, MD 20899**

January 1991

# **90-3**

**U.S. DEPARTMENT OF COMMERCE  
Robert A. Mosbacher, Secretary  
NATIONAL INSTITUTE OF STANDARDS  
AND TECHNOLOGY  
John W. Lyons, Director**

**NIST**



**Center for Electronics and  
Electrical Engineering**

# **Technical Progress Bulletin**

Covering Center Programs,  
July to September 1990,  
with 1991 CEEE Events Calendar

**U.S. DEPARTMENT OF COMMERCE  
National Institute of Standards  
and Technology  
Center for Electronics and  
Electrical Engineering  
Semiconductor Electronics Division  
Gaithersburg, MD 20899**

January 1991

# **90-3**



**U.S. DEPARTMENT OF COMMERCE  
Robert A. Mosbacher, Secretary  
NATIONAL INSTITUTE OF STANDARDS  
AND TECHNOLOGY  
John W. Lyons, Director**

This is the thirty-second issue of a quarterly publication providing information on the technical work of the National Institute of Standards and Technology (formerly the National Bureau of Standards) Center for Electronics and Electrical Engineering. This issue of the CEEE Technical Progress Bulletin covers the third quarter of calendar year 1990.

Organization of Bulletin: This issue contains abstracts for all Center papers released for publication by NIST in the quarter and citations and abstracts for Center papers published in the quarter. Entries are arranged by technical topic as identified in the table of contents and alphabetically by first author under each subheading within each topic. Unpublished papers appear under the subheading "Released for Publication." Papers published in the quarter appear under the subheading "Recently Published." Following each abstract is the name and telephone number of the individual to contact for more information on the topic (usually the first author). This issue also includes a calendar of Center conferences and workshops planned for calendar year 1991 and list of sponsors of the work.

Center for Electronics and Electrical Engineering: Center programs provide national reference standards, measurement methods, supporting theory and data, and traceability to national standards.

The metrological products of these programs aid economic growth by promoting equity and efficiency in the marketplace, by removing metrological barriers to improve productivity and innovation, by increasing U.S. competitiveness in international markets through facilitation of compliance with international agreements, and by providing technical bases for the development of voluntary standards for domestic and international trade. These metrological products also aid in the development of rational regulatory policy and promote efficient functioning of technical programs of the Government.

The work of the Center is divided into two major programs: the Semiconductor Technology Program, carried out by the Semiconductor Electronics Division in Gaithersburg, MD, and the Signals and Systems Metrology Program, carried out by the Electricity Division in Gaithersburg and the Electromagnetic Fields and Electromagnetic Technology Divisions in Boulder, CO. Key contacts in the Center are given on the back cover; readers are encouraged to contact any of these individuals for further information. To request a subscription or for more information on the Bulletin, write to CEEE Technical Progress Bulletin, National Institute of Standards and Technology Metrology Building, Room B-358, Gaithersburg, MD 20899 or call (301) 975-2220.

Center sponsors: The Center Programs are sponsored by the National Institute of Standards and Technology and a number of other organizations, in both the Federal and private sectors; these are identified on page 43.

Note on Publication Lists: Guides to earlier as well as recent work are the publication lists covering the work of each division. These lists are revised and reissued on an approximately annual basis and are available from the originating division. The current set is identified in the Additional Information section, page 36.

TABLE OF CONTENTS

INTRODUCTION . . . . . inside front cover

SEMICONDUCTOR TECHNOLOGY PROGRAM . . . . . 2

  Silicon Materials . . . . . 2

  Compound Semiconductor Materials . . . . . 2

  Analysis Techniques . . . . . 3

  Dimensional Metrology . . . . . 3

  Power Devices . . . . . 3

  Photodetectors . . . . . 4

  Integrated Circuit Test Structures . . . . . 5

  Device Physics and Modeling . . . . . 5

  Insulators and Interfaces . . . . . 6

  Packaging . . . . . 8

  Microfabrication Technology . . . . . 8

  Other Semiconductor Metrology Topics . . . . . 9

SIGNALS & SYSTEMS METROLOGY PROGRAM . . . . . 10

FAST SIGNAL ACQUISITION, PROCESSING, & TRANSMISSION . . . . . 10

  Waveform Metrology . . . . . 10

  DC & Low Frequency Metrology . . . . . 11

  Fundamental Electrical Measurements . . . . . 13

  Cryoelectronic Metrology . . . . . 14

  Pulse Power Metrology . . . . . 16

  Antenna Metrology . . . . . 16

  Microwave & Millimeter-Wave Metrology . . . . . 16

  Optical Fiber Metrology . . . . . 17

  Optical Fiber Sensors . . . . . 18

  Electro-Optic Metrology . . . . . 20

  Electromagnetic Properties . . . . . 21

  Other Fast Signal Topics . . . . . 21

ELECTRICAL SYSTEMS . . . . . 23

  Power Systems Metrology . . . . . 23

  Superconductors . . . . . 27

  Magnetic Materials & Measurements . . . . . 33

  Other Electrical Systems Topics . . . . . 35

ELECTROMAGNETIC INTERFERENCE . . . . . 36

  Radiated Electromagnetic Interference . . . . . 36

ADDITIONAL INFORMATION . . . . . 36

1991 IEEE CALENDAR . . . . . 42

AUTHOR LIST . . . . . 43

KEY CONTACTS IN CENTER, CENTER ORGANIZATION . . . . . back cover

## SEMICONDUCTOR TECHNOLOGY PROGRAM

Silicon Materials

Released for Publication

Geist, J., Schaefer, A.R., Song, J-F., Wang, Y.H., and Zalewski, E.F., **An Accurate Value for the Absorption Coefficient of Silicon at 633 nm.**

High-accuracy transmission measurements at an optical wavelength of 633 nm and mechanical measurements of the thickness of a 13- $\mu\text{m}$  thick silicon-crystal film have been used to calculate the absorption and extinction coefficients of silicon at 633 nm. The results are  $3105 \pm 62 \text{ cm}^{-1}$  and  $0.01564 \pm 0.00031$ , respectively. These results are about 15% less than current handbook data for the same quantities, but are in good agreement with a recent fit to one set of data described in the literature.

[Contact: Jon Geist, (301) 975-2066]

Compound Semiconductor Materials

Released for Publication

Littler, C.L., Loloee, M.R., Zawadzki, W., and Seiler, D.G., **Bound Hole Excitations in p-Hg<sub>0.76</sub>Cd<sub>0.24</sub>Tc**, to be published in the Proceedings of the 20th International Conference on the Physics of Semiconductors, Thessaloniki, Greece, August 6-10, 1990.

Bound-hole transitions originating from a deep level to light-hole Landau levels have been observed for the first time in HgCdTe. Resonances have been seen in the photovoltaic response of a p-type Hg<sub>0.76</sub>Cd<sub>0.24</sub>Tc sample subjected to CO<sub>2</sub> laser radiation. The transitions are well described by the Pidgeon-Brown energy band model, yielding an activation energy of  $32 \pm 2 \text{ meV}$  above the valence band edge for the deep level.

[Contact: David G. Seiler, (301) 975-2081]

Littler, C.L., Yoon, I.T., Song, X.N., Zawadzki, W., Pfeffer, P., and Seiler, D.G., **Orbital and Spin Anisotropy of Conduction Electrons in InSb**, to be published in the Proceedings of the 20th International Conference on the Physics of Semiconductors, Thessaloniki, Greece, August 6-10, 1990.

The anisotropy of the orbital and spin properties of conduction electrons in InSb has been measured simultaneously for the first time using a cyclotron-resonance-type experiment. A novel approach was used to measure precisely small shifts of the resonant field positions with respect to the crystal axes -- the cyclotron resonance signals were detected at the same time from two differently oriented samples. The data have been described using a five-level k·p energy band model, which accounts for both the nonparabolicity and anisotropy of the conduction band in III-V compounds in the presence of a magnetic field.

[Contact: David G. Seiler, (301) 975-2081]

Myers, D.R., Dawson, L.R., Klem, J.F., Brennan, T.M., Hammons, B.E., Simons, D.S., Comas, J., and Pellegrino, J.G., **Unintentional Indium Incorporation in GaAs Grown by Molecular-Beam Epitaxy.**

We have characterized unintentional indium incorporation into GaAs grown by molecular-beam epitaxy in a variety of commercial molecular-beam epitaxy systems. We find that the unintentional indium-doping level in the epitaxial GaAs during growth is more a function of mounting technique and prior machine history than of the manufacturer's design. The indium doping detected in the epitaxial GaAs for substrates that only partially obscure an indium-bearing mount is equal to levels reported to result in minimum defect densities and narrowest photoluminescence linewidths in In-doped GaAs.

[Contact: Joseph G. Pellegrino, (301) 975-2123]

Analysis Techniques

Released for Publication

McKeown, D.A., **XANES of Transition Metal Zinc-Blende Semiconductors**, to be published in the Proceedings of the Sixth International Conference on X-Ray Absorption Fine Structure, York, United Kingdom, August 5-11, 1990.

XANES (X-ray absorption near-edge structure) is known to be sensitive to both the arrangement of atoms around, as well as the atomic states of, the absorbing atom. Therefore, it is not surprising that XANES data, collected on compounds having different arrangements of atoms around the absorbing atom, can have very different features. In this study, XANES data were gathered for three transition metals: Fe and Cu in chalcopyrite ( $\text{CuFeS}_2$ ), and Zn in sphalerite ( $\text{ZnS}$ ), where all three cations are in nearly identical atomic environments (similar to the zinc-blende type structures in III-V semiconductors). Since the environments are similar, any change in the XANES should, to first approximation, be due entirely to atomic effects of the absorbing atom. The rationale behind this study is to see if any changes in the near-edge data can be assigned to electronic transitions of the absorbing atom; this may be useful for interpreting XANES for III-V semiconductors. Previously, Zn, Cu, and Fe edges were presented separately, but no comparisons or calculations have been made for all three edges.

Contact: David A. McKeown, (301) 975-095]

Dimensional Metrology

Recently Published

Postek, M.T., Keery, W.J., and Frederick, N.V., **Low-Profile Microchannel-Plate Electron Detector System for SEM**, Proceedings of the XIIth International Congress for Electron Microscopy, Seattle, Washington, August 12-18, 1990, pp. 378-379 (1990).

One main impetus of present-day scanning electron microscopy is in the low accelerating voltage mode. This mode of operation is useful for nondestructive inspection, especially in the on-line inspection and metrology of semiconductor samples. Today, the majority of the scanning electron microscopes used in nondestructive inspection utilize the standard Everhart/Thornley (E/T) detector or a modification of this detector as the main detection system. The E/T detector, although extremely efficient, suffers from poor signal-to-noise ratio at low accelerating voltages. This type of detector also suffers from alignment difficulties especially where linewidth measurement for semiconductor applications is concerned because of the uneven distribution of the collection field, which is possible especially if the detector is not located in a plane of symmetry of the specimen and electron beam. These limitations and others have recently led investigators to reconsider the design of secondary electron detection systems, especially for low accelerating voltage and metrological applications.

[Contact: Beverly Wright, (301) 975-2166]

Power Devices

Recently Published

Berning, D.W., **Semiconductor Measurement Technology: A Programmable Reverse-Bias Safe Operating Area Transistor Tester**, NIST Special Publication 400-87 (August 1990).

This document describes the circuits and construction of a transistor turn-off breakdown tester. Principles of operation for various circuits in the tester are discussed, as well as those for the complete system. Construction notes are given with layout guidelines. Complete circuit schematics are included, and details of constructions of special parts used in the tester are furnished. Specifications and performance data are also included in this document.

Power Devices (cont'd.)

[Contact: David W. Berning, (301) 975-2069]

Oettinger, F.F., and Blackburn, D.L., **Semiconductor Measurement Technology: Thermal Resistance Measurements**, NIST Special Publication 400-86 (July 1990).

This Special Publication reviews the thermal properties of power transistors and integrated circuits and discusses methods for characterizing these properties. The discrete devices discussed include bipolar transistors and metal-oxide-semiconductor field-effect-transistors. Measurement problems common to these devices, such as deciding the reason a particular measurement is required, adequate reference temperature control, selection of a temperature-sensitive electrical parameter, and separation of electrical and thermal effects during measurement, are addressed. Due to the inherent difficulties in measuring and analyzing the thermal properties of active integrated circuits, an approach using specifically designed thermal test chips for evaluation of new die attachment and packaging schemes is finding wide acceptance in the industry. In this Special Publication, indirect (i.e., electrical) measurements, direct (e.g., infrared) measurements, and computer simulation techniques for thermally characterizing integrated circuits are discussed in terms of their usefulness in characterizing VLSI packages.

[Contact: Frank F. Oettinger, (301) 975-2054]

Photodetectors

Released for Publication

Geist, J., and Novotny, D.B., **Low-Contrast Thermal Resolution Test Targets: A New Approach.**

A new type of thermal resolution test target optimized to minimize the effects of lateral thermal gradients at low

thermal contrast is described. This target consists of thin-film inconel heater strips over an etched silicon substrate bonded to an aluminum heat sink. A simple, finite-difference model is used to study how variations in target construction and materials affect the generated thermal resolution test pattern. The construction, testing, and use of this type of target to extend the lower end of the contrast range of conventional target are described.

[Contact: Jon Geist, (301) 975-2066]

## Recently Published

Geist, J., Gardner, J.L., and Wilkinson F.J., **Surface-Field-Induced Feature in the Quantum Yield of Silicon near 3.5 eV**, Physical Review B, Vol. 42, No. 2, pp. 1262-1267 (15 July 1990).

A broad feature near 3.5 eV was observed in the internal quantum efficiency spectra of various silicon photodiodes. This appears to be the first time this feature has been reported. The feature was clearly resolved in spectra from photodiodes with strong surface fields at the oxide-silicon interface, but was small enough to preclude observation in published spectra for photodiodes with nearly flat-band conditions at the interface. The feature is attributed to a local maximum in the quantum yield for electron-hole pair production that is expected at direct transitions in the vicinity of the  $\Gamma$  point in the silicon band structure. Qualitative arguments suggest that the magnitude of the feature increases with increasing surface field due to field-assisted impact ionization, and in the case of depleted surfaces, also due to band-gap narrowing in the surface depletion region.

[Contact: Jon Geist, (301) 975-2066]

Geist, J., Migdall, A., and Baltes, H., **Shape of the Silicon Absorption Coefficient Spectrum Near 1.63 eV**, Applied Optics, Vol. 29, No. 24, pp. 3548-3552 (20 August 1990).

We report high-precision, high-spectral

Photodetectors (cont'd.)

resolution measurements of the absorption coefficient of silicon in the region from 1.61 to 1.65 eV. Our results, together with a simulation of the effect of a second indirect transition on the absorption coefficient of silicon, suggest that features reported by Forman et al. (1974) and by Hulthen and Nilsson (1976) around 1.63 eV are not real, and that the second indirect transition in silicon has yet to be detected in absorption coefficient spectra.

[Contact: Jon Geist, (301) 975-2066]

Kohler, R., Luther, J.E., and Geist, J., **Reflectometer for Measurements of Scattering from Photodiodes and Other Low Scattering Surfaces**, Applied Optics, Vol. 29, No. 21, pp. 3130-3134 (20 July 1990).

We have designed and tested a simple instrument to measure the diffuse reflectance of good quality optical surfaces such as the surfaces of semiconductor detectors. Measurements have been performed on silicon-photodiodes and on a sample of known reflectance at two different wavelengths.

Contact: Jon Geist, (301) 975-2066]

Integrated Circuit Test Structures

Released for Publication

Cresswell, M.W., Khera, D., Linholm, L.W., and Schuster, C. E., **Classification of Electrical Test Data Patterns Extracted From Semiconductor Wafers Using a Directed Graph.**

The application of the subject of this paper is to support the training of expert systems for process diagnosis and yield and/or reliability prediction in semiconductor manufacturing. The technique itself is the use of a directed graph for partitioning an electrically tested set of fully, or partially, processed semiconductor wafers into groups. The partitioning is performed on the basis of the test data extracted from

die sites across the wafer surface such that, after partitioning, wafers within each group have similar distributions of electrical test data across their surfaces. The wafers thus partitioned are referred to as the training set. The directed graph that is developed during partitioning subsequently enables the classification of an incoming wafer that is not included in the original training set to one of the groups established by the partitioning. This classification provides the estimation of some property of interest of the incoming wafer and is characterized by an efficient search for, and recognition of, existing test data patterns most similar to the incoming wafer test pattern. Intralevel isolation test structure data are used here to illustrate the construction of the directed graph from a starting database, and the principles of its operation and application. The techniques are, of course, valid for any available test measurement, whether extracted from a test structure or an actual integrated circuit device.

[Contact: Michael W. Cresswell, (301) 975-2072]

Device Physics & Modeling

Recently Published

Bennett, H.S., and Lowney, J.R., **Physics for Numerical Simulation of Silicon and Gallium Arsenide Transistors**, Solid-State Electronics, Vol. 33, No. 6, pp. 675-691 (1990).

The motivation for using computers to simulate the electrical characteristics of transistors is discussed. Our work and that of others in the area of device physics and modeling is described. We compare conventional device physics with an alternative approach to device physics that is more directly traceable to quantum-mechanical concepts. We then apply this new approach to quasi-neutral regions, space-charge regions, and regions with high levels of carrier injection. The limits for using theoretical results from uniform media in numerical simula-

Device Physics & Modeling (cont'd.)

tions of devices with large concentration gradients are discussed. New calculations of the effective intrinsic carrier concentrations for gallium arsenide and silicon are also given. We conclude with examples of applying quantum-mechanically-based device physics to energy band diagrams for heterojunction bipolar transistors, MOS capacitors, and unirradiated and irradiated homojunction bipolar transistors.

[Contact: Herbert S. Bennett, (301) 975-2053]

Kim, J.S., **A New Method of Extracting the Channel Length from the Gate Current of p-Channel MOSFETs** [original title: Determining the Channel Length of MOSFET's From the Fowler-Nordheim Tunneling Current], *Solid-State Electronics*, Vol. 33, No. 8, pp. 1097-1107 (1990).

A new method for determining the channel length of MOSFETs is proposed and experimentally tested. The method is based on the proportionality between the channel area and the body-to-gate current in the Fowler-Nordheim tunneling regime. The new method appears to be superior to two conventionally used techniques, namely, the channel-conductance and the gate-capacitance methods, since it circumvents measurement interferences due to the parasitics encountered in these methods.

[Contact: Jin S. Kim, (301) 975-2238]

Insulators and Interfaces

Released for Publication

Mattis, R.L., **SPARCOL: A Front End for the MAIN2 Program**, to be published as NISTIR 4426.

SPARCOL is an interactive program which serves as a front-end to the MAIN2 and MAIN2R computer programs. SPARCOL (pronounced "sparkle") stands for SPECTROSCOPIC ellipsometry AND reflectance for CHARACTERIZATION OF layers. It consists of a FORTRAN-77 program and a VMS DCL

command procedure. SPARCOL is used to prepare the X.DAT and X.INN files required by MAIN2 and MAIN2R, and to give these files user-defined names. Although these two files can be created using a text editor, the user may find it helpful to prepare them using SPARCOL.

[Contact: Richard L. Mattis, (301) 975-2235]

Mayo, S., Lowney, J.R., Roitman, P., and Novotny, D.B., **Persistent Photoconductivity in SIMOX Film Structures**, to be published as a Technical Abstract of the 1990 IEEE SOS/SOI Technology Conference, Key West, Florida, October 2-4, 1990.

Photoinduced transient spectroscopy (PITS) was used to measure the persistent photoconductive (PPC) response in film resistors fabricated on two different commercial n-type SIMOX (separation by implanted oxygen) wafers. A broadband, single-shot, flashlamp-pumped dye laser pulse was used to photoexcite interband electrons in the film, and the decay in the induced excess carrier population was measured at temperatures in the 60- to 220-K range. The post-illumination conductivity transients observed show PPC signals exhibiting nonexponential character. They were recorded for periods of time up to 30 s at constant temperature. The photoconductive data from these film resistors are analyzed by using the Queisser and Theodorou potential barrier model, and a logarithmic time decay dependence is confirmed for the first time in SIMOX material. The sensitivity of PITS is demonstrated to be appropriate for characterization of the SIMOX interface structure and for material qualification.

[Contact: Santos Mayo, (301) 975-2045]

Roitman, P., Edelstein, M., Krause, S., and Visitserngtrukul, S., **Residual Defects in SIMOX: Threading Dislocations and Pipes**, to be published as a Technical Abstract of the 1990 IEEE SOS/SOI Technology Conference, Key West, Florida, October 2-4, 1990.

In the past few years, due to improved

Insulators & Interfaces (cont'd.)

control of the ion implantation process and improved annealing sequences, a qualitative improvement has been realized in the structural quality of SIMOX films. The dense network of oxide precipitates and threading dislocations in the top silicon can be annealed out, reducing the dislocation density from  $\approx 10^{10}/\text{cm}^2$  to  $\approx 10^5/\text{cm}^2$  or less. CMOS transistors and circuits have been successfully fabricated in this material. However, bipolar devices are sensitive to defect densities in this range, as is VLSI yield. Therefore, the defect density must be monitored and reduced. We discuss below some techniques for monitoring dislocations and stacking faults in SIMOX films. Also, a different type of defect, a silicon "pipe" running through the buried oxide has been observed. The origin of these defects and a technique for detecting them is described.

[Contact: Peter Roitman, (301) 975-2077]

## Recently Published

Kopanski, J.J., MIS Capacitor Studies on Silicon Carbide Single Crystals: Final Report for May 8, 1989 to November 8, 1989, NISTIR 4352 (July 1990).

In this continuation of previous work, cubic SiC metal-insulator-semiconductor (MIS) capacitors with thermally grown or chemical-vapor-deposited (CVD) insulators were characterized by capacitance-voltage (C-V), conductance-voltage (G-V), and current-voltage (I-V) measurements. The purpose of these measurements was to determine the four charge densities commonly present in an MIS capacitor (oxide fixed charge,  $N_f$ ; interface trap level density,  $D_{it}$ ; oxide trapped charge,  $N_{ot}$ ; and mobile ionic charge,  $N_m$ ) and to determine the stability of the device properties with electric field stress and temperature. It was found that an electric field stress would alter the shape of the SiC MIS capacitor C-V characteristics. A negative voltage stress at room temperature would result

in a negative shift of the C-V characteristics, indicating the creation of positive charge in the oxide. A positive voltage stress at room temperature resulted in no detectable shift of the C-V curve. The sense of these shifts in the C-V curves is the same as that observed for the "slow trapping" instability often observed in silicon and other semiconductor-based MIS capacitors. From the shift in the C-V characteristics at the midgap point, it was found that a negative voltage stress could increase  $N_{ot}$  by as much as  $5 \times 10^{11} \text{ cm}^{-2}$ . A voltage stress was also found to increase  $D_{it}$  by as much as 25%. The mobile ionic charge density was determined from a series of elevated temperature bias stress measurements.  $N_m$  for the capacitors in this study ranged from less than  $1 \times 10^{11}$  to  $4 \times 10^{11} \text{ cm}^{-2}$ . It was found that increasing the temperature would also change the shape of the C-V characteristics, indicating an increase in the number of active interface traps. The resistivity and breakdown field of various insulators on SiC were determined from the I-V characteristics of the capacitors. For capacitors with thermal oxide insulating layers, the average resistivity was about  $10^{16} \Omega\text{-cm}$  and the average electric breakdown field was  $3.3 \times 10^6 \text{ V/cm}$ . Fowler-Nordheim tunneling was identified as the charge conduction mechanism for thermal oxide layers on cubic SiC. The barrier height between n-type SiC and  $\text{SiO}_2$  for the tunneling of electrons was determined to be  $1.8 \pm 0.1 \text{ eV}$  by fitting the Fowler-Nordheim formula to the observed I-V curve. Finally, some deep-level transient capacitance measurements were attempted on some of the SiC MIS capacitors and on Au on SiC Schottky diodes. In the conclusions of this report, a comprehensive summary of the electrical properties of cubic SiC MIS capacitors is presented.

[Contact: Joseph J. Kopanski, (301) 975-2089]

Miyano, K.E., Kendelewicz, T., Cao, R., Spindt, C.J., Lindau, I., Spicer, W.E., and Woicik, J.C., Morphology and Barrier-Height Development of Bi/InP(110)

Insulators & Interfaces (cont'd.)

**Interfaces**, Physical Review B, Vol. 42, No. 5, pp. 3017-3023 (15 August 1990).

The development of the interface between cleaved n- and p-type InP(110) substrates and overlayers of Bi has been studied in the coverage range of 0.01 to 10 monolayers with use of soft-X-ray photoemission spectroscopy. The attenuation and narrowing of the substrate In 4d and P 2p core-level spectra, as well as the lineshape development of the adatom Bi 5d signal, indicate that the morphology is of the Stranski-Krastanov type, as has been verified previously for Sb and Bi overlayers on GaAs(110). Specifically, the Bi grows in ordered two-dimensional patches that merge at one monolayer coverage, and beyond this coverage the deposited adatoms form three-dimensional clusters. The band bending as measured from energy shifts of the In 4d and P 2p spectra approaches midgap near 0.3 monolayer coverage, but between 0.3 and 1.0 monolayer, the band bending for both doping types exhibits a reversal. The reduction in band bending in this deposition regime suggests that some of the submonolayer band bending is induced by states originating at the periphery of the two-dimensional Bi patches. The Bi 5d core-level position provides a local measurement of the surface-Fermi-level position directly beneath these Bi patches: specifically, the absence of Bi 5d shifts suggests that these patches are regions of strong local depletion at coverages as low as 0.01 monolayer. As the three-dimensional Bi clusters develop for depositions exceeding one monolayer, the n- and p-type-surface Fermi-level positions proceed toward 0.75 eV above the valence-band maximum, a position which has been reported for other unreacted metal-InP interfaces. However, the Sb/InP interface, which exhibits a morphology very similar to Bi/InP, gives a barrier height 0.4 eV higher in the gap. Thus, it is observed that the interfacial states at these unreacted and ordered interfaces between such semimetals and InP are strongly dependent on

the specific overlayer material.

[Contact: Charles E. Bouldin, (301) 975-2046]

Packaging

## Recently Published

Oettinger, F.F., and Blackburn, D.L., **Semiconductor Measurement Technology: Thermal Resistance Measurements**, NIST Special Publication 400-86 (July 1990).

This Special Publication reviews the thermal properties of power transistors and integrated circuits and discusses methods for characterizing these properties. The discrete devices discussed include bipolar transistors and metal-oxide-semiconductor field-effect-transistors. Measurement problems common to these devices, such as deciding the reason a particular measurement is required, adequate reference temperature control, selection of a temperature-sensitive electrical parameter, and separation of electrical and thermal effects during measurement, are addressed. Due to the inherent difficulties in measuring and analyzing the thermal properties of active integrated circuits, an approach using specifically designed thermal test chips for evaluation of new die attachment and packaging schemes is finding wide acceptance in the industry. In this Special Publication, indirect (i.e., electrical) measurements, direct (e.g., infrared) measurements, and computer simulation techniques for thermally characterizing integrated circuits are discussed in terms of their usefulness in characterizing VLSI packages.

[Contact: Frank F. Oettinger, (301) 975-2054]

Microfabrication Technology

## Released for Publication

Dagata, J.A., Schneir, J., Harary, H.H., Bennett, J., and Tseng, W., **Pattern Generation on Semiconductor Surfaces by a Scanning Tunneling Microscope Operating**

Microfabrication Technology (cont'd.)

in Air, to be published in the Proceedings of the Scanning Tunneling Microscopy '90/Nanometer Scale Science and Technology Symposium I, Baltimore, Maryland, July 23-27, 1990.

Recent results employing scanning tunneling microscope-based techniques for the generation of nanometer-scale patterns on passivated semiconductor surfaces are presented. Preparation and characterization of hydrogen-passivated silicon and sulfur-passivated gallium arsenide surfaces are described, and the determination of the chemical and morphological properties of the patterned regions by scanning electron microscopy and time-of-flight secondary ion mass spectrometry are discussed. Our recent demonstration that ultra-shallow, oxide features written by an STM can serve as an effective mask for selective-area GaAs heteroepitaxy on silicon is used to illustrate the requirements necessary for the realization of a unique, STM-based nanotechnology.

Contact: Wen F. Tseng, (301) 975-5291]

Other Semiconductor Metrology Topics

## Recently Published

Lee, K.C., **The Fabrication of Thin, Free-standing, Single-Crystal, Semiconductor Membranes**, Journal of the Electrochemical Society, Vol. 137, No. 8, pp. 2556-2574 (August 1990).

Free-standing, single-crystal, semiconductor membranes with thicknesses in the range of a few tens of nanometers to tens of microns are of increasing technological interest today. Their applications range from high-speed electronic devices to electromechanical devices and pressure sensors. This review paper identifies two general classes of techniques for producing such thin membranes: dissolution of single-crystal wafers and direct growth of single-crystal membranes. Numerous specific techniques in each general class are discussed. The discus-

sion of each technique includes a brief explanation of the reason why it works, a description of the actual experimental implementation, an analysis of the range of thicknesses that can be produced, and the crystalline and electrical quality of the membranes. Unusual difficulties with implementing a technique or special advantages of a technique are also noted. Since this review is intended to aid in the selection of a technique for producing thin semiconductor membranes when one has a particular application in mind, note is made of those applications for which the membranes produced with each technique are particularly well suited. [Contact: Kevin C. Lee, (301) 975-4326]

Littler, C.L., Zawadzki, W., Loloee, M.R., Song, X.N., and Seiler, D.G., **Phonon-Assisted Magneto-Donor Optical Transitions in n-InSb**, (Proceedings of the International Conference on Narrow-Gap Semiconductors and Related Materials, Gaithersburg, Maryland, June 12-15, 1989), Semicond. Sci. Technol., Vol. 5, No. 3S, pp. S169-S171 (1990).

We have observed and described new optical transitions between magneto-donor states in InSb assisted by optic phonon emission. The phonon-assisted transitions provide a unique opportunity to investigate high excited states of the magneto-Coulomb system. High-resolution data reveal the presence of excited magneto-donor states belonging to the same Landau sub-band.

[Contact: David G. Seiler, (301) 975-2081]

Scace, R.I., **Semiconductor Technology for the Non-Technologist, Second Edition**, NISTIR 4414 (September 1990).

The properties of semiconductor materials, the methods of processing them, and the solid-state products made from them are described in terms intended to be understandable by the lay person. The semiconductor industry has grown at a rate of 17 percent per year compounded for the last thirty years. Its products have declined in unit cost by a factor of

Other Semiconductor Topics (cont'd.)

4.7 in current dollars (a factor of 18 in constant dollars) in the same period, irrespective of the vastly increased capabilities of today's products. This very satisfactory but anomalous behavior has attracted the interest of many who are not familiar with the technology of the industry, yet who need to have some understanding of it. This report is intended to help meet that need.

[Contact: Robert I. Scace, (301) 975-2220]

Seiler, D.G., and Littler, C.L., **International Conference on Narrow-Gap Semiconductors and Related Materials**, Gaithersburg, MD, June 12-15, 1989 [original title: **Narrow Gap Semiconductors: Perspectives and State of the Art**], *Journal of Research of the National Institute of Standards and Technology*, Vol. 95, No. 4, pp. 469-481 (July-August 1990).

The Semiconductor Electronics Division at the National Institute of Standards and Technology hosted an International Conference on Narrow-Gap Semiconductors and Related Materials in Gaithersburg, Maryland on June 12-15, 1989. A brief background on narrow-gap semiconductors is given in this paper, along with an overview of the conference itself. The major section of this report is devoted to highlights from each of the invited papers in order to give a perspective on this field of semiconductor research and technology. The Conference Proceedings were published as a special issue of *Semiconductor Science and Technology* (IOP Publishing, Bristol, 1990).

[Contact: David G. Seiler, (301) 975-2074]

Seiler, D.G., and Littler, C.L., **Narrow-Gap Semiconductors and Related Materials**, (Editors), Adam Hilger, Bristol, England (1990).

The special characteristics of narrow-gap semiconductors have long been recognized, not only for their interesting

physical effects, but also for their technological applications. Such materials are found across a wide range of elements, compounds, and alloys. The International Conference on Narrow-Gap Semiconductors and Related Materials (National Institute of Standards and Technology, Gaithersburg, Maryland) reviewed past research into the physics of both materials and devices, and summarized the present position, in the light of recent rapid developments in the semiconductor field. This major conference, the first of its kind since 1981, drew together 159 delegates from 14 countries. Invited reviews and invited and contributed papers covered II-VI, III-V and IV-VI compounds and various alloys. Topics considered ranged from the characterization of artificially structured materials to the physics of infrared detector devices, as well as a review of high- $T_c$  superconductors for infrared detection; this diversity is reflected in the reviews and papers presented here. This book will be of value to all scientists and engineers interested in narrow-gap semiconductors and needing to keep up to date with the rapid advances in this area.

[Contact: David G. Seiler, (301) 975-2081]

**SIGNALS & SYSTEMS METROLOGY PROGRAM****FAST SIGNAL ACQUISITION, PROCESSING, AND TRANSMISSION**Waveform Metrology

Released for Publication

Oldham, N.M., and Nelson, T.L., **Influence of Nonsinusoidal Waveforms on Voltmeters, Ammeters, and Phasemeters**, to be published in the *Harmonics Tutorial Proceedings*, IEEE Winter Power Meeting, New York, New York, February 3-7, 1991.

The operating principles of various voltmeters, ammeters, and phasemeters are described. The results of tests of these instruments at different levels of distortion indicate that phasemeters are

Waveform Metrology (cont'd.)

subject to large, often unpredictable errors while most voltmeters and ammeters respond to the rms value, independent of waveshape.

[Contact: Nile M. Oldham, (301) 975-2408]

Souders, T.M., and Stenbakken, G.N., **A Comprehensive Approach for Testing Analog and Mixed-Signal Devices**, to be published in the 1990 Proceedings of the International Test Conference, Washington, D.C., September 10-12, 1990.

An approach is presented for optimizing the testing of analog and mixed-signal devices. The entire process is performed with algebraic operations on an appropriate model. The paper demonstrates how this is accomplished using simple calls with public-domain software. Examples of test results achieved using this approach are included.

[Contact: T. Michael Souders, (301) 975-2406]

#### Recently Published

Bell, B.A., **Standards for Waveform Metrology Based on Digital Techniques**, Journal of Research of the National Institute of Standards and Technology, Vol. 95, No. 4, pp. 377-405 (July-August 1990).

Over the last decade, the use of digital synthesis and sampling techniques for generating and measuring electrical waveforms has increased dramatically with the availability of improved digital-to-analog and analog-to-digital converters and related devices. With this evolution has come the need for physical laboratory standards and test methods to support the performance specifications of digital devices and the instruments in which they are used. This article describes the research and development at NIST of several laboratory standards and test systems that utilize "digital technology" for characterizing data converters and for implementing various waveform syn-

thesis and sampling instruments.

[Contact: Barry A. Bell, (301) 975-2419]

Waltrip, B.C., and Oldham, N.M., **Performance Evaluation of a New Audio-Frequency Power Bridge**, Digest of the 1990 Conference on Precision Electromagnetic Measurements, Ottawa, Canada, June 11-14, 1990, pp. 142-143 (1990).

Several techniques for measuring active and reactive power in the 50-Hz to 20-kHz frequency range are described. The approaches include: (1) the development of a high-precision sampling wattmeter using a resistive attenuator, a shunt, and two commercially available sampling voltmeters configured as a dual-channel equivalent-time sampler; (2) the development of another high-precision sampling wattmeter using the same shunt and attenuator, a high-impedance, wideband differential amplifier, and a commercially available, dual-channel, direct-sampling waveform analyzer; (3) for zero power factor measurements, the use of a digital generator to produce precise phase shifts from  $+\pi/2$  to  $-\pi/2$ ; and (4) the use of simultaneous thermal voltage and current measurements for unity power factor measurements. These approaches were developed to evaluate a new high-accuracy, audio-frequency power bridge that is based on ac voltage and impedance measurements.

[Contact: Bryan C. Waltrip, (301) 975-2438]

DC & Low Frequency Metrology

#### Released for Publication

Guang-qiu, T., and Xiu-ye, X., **A Wide Band Active Inductive Shunt**.

An active inductive shunt with high accuracy and wide frequency range is introduced in this paper. The new shunt can be used in the audio frequency band. It has a wide current ratio (0.01 to 1) and good loading capacity. If the external burden of the inductive shunt is an ac standard resistor, it will become

DC & Low Frequency Metrology (cont'd.)

an ac current-to-voltage transducer that can be used in many electromagnetic measurements. The relative uncertainty ( $3\sigma$ ) in the current ratio of the new shunt is  $(1 + j1)$  ppm to  $(8 + j8)$  ppm over the frequency range from 40 Hz to 10 kHz.

[Contact: Barry A. Bell, (301) 975-2419]

## Recently Published

Cage, M.E., Yu, D.Y., Jeckelmann, B.M., Steiner, R.L., and Duncan, R.V., **Investigating the Use of Multimeters to Measure Quantized Hall Resistance Standards**, Digest of the 1990 Conference on Precision Electromagnetic Measurements, Ottawa, Canada, June 11-14, 1990, pp. 332-333 (1990).

A new generation of digital multimeters was used to compare the ratios of the resistances of wire-wound reference resistors and quantized Hall resistances. The accuracies are better than 0.1 ppm for ratios as large as 4:1 if the multimeters are calibrated with a Josephson array.

[Contact: Marvin E. Cage, (301) 975-4248]

Field, B.F., and Oldham, N.M., **Digital Source for a New Impedance Bridge**, Digest of the 1990 Conference on Precision Electromagnetic Measurements, Ottawa, Canada, June 11-14, 1990, pp. 24-25 (1990).

A digitally-synthesized source has been designed to provide two sine wave outputs with an accurately known adjustable phase shift in the second channel for use with a proposed new impedance bridge.

[Contact: Bruce F. Field, (301) 975-4230]

Hamilton, C.A., Burroughs, C.J., and Chieh, K., **Operation of NIST Josephson Array Voltage Standards** [original title: Operation of Josephson-Array Voltage Standards], Journal of Research of the

National Institute of Standards and Technology, Vol. 95, No. 3, pp. 219-235 (May-June 1990).

This paper begins with a brief discussion of the physical principles and history of Josephson voltage standards. The main body of the paper deals with the practical details of the array design, cryoprobe construction, bias source requirements, adjustment of the system for optimum performance, calibration algorithms, and an assessment of error sources.

[Contact: Clark A. Hamilton, (303) 497-3740]

Kinard, J.R., Huang, D.X., and Novotny, D.B., **Hybrid Construction of Multijunction Thermal Converters**, Digest of the 1990 Conference on Precision Electromagnetic Measurements, Ottawa, Canada, June 11-14, 1990, pp. 62-63 (1990).

Using thin-film and thick-film technologies, multijunction thermal converters have been designed for frequencies ranging from audio up to tens of megahertz and for heater currents from a few milliamperes up to hundreds of milliamperes. This paper describes these designs and the early production of prototype converters.

[Contact: Joseph R. Kinard, (301) 975-4250]

Kinard, J.R., Huang, D.X., and Rebuldela, G., **RF-DC Differences of Thermal Voltage Converters Arising from Input Connectors**, Digest of the 1990 Conference on Precision Electromagnetic Measurements, Ottawa, Canada, June 11-14, 1990, pp. 280-281 (1990).

The radiofrequency-dc differences of thermal voltage converters caused by skin effect and transmission line effects of different length input structures have been previously studied. Discrepancies do exist, however, between simple mathematical models and measured results for commonly used input connectors. This paper reports a study of these discrepancies.

DC & Low Frequency Metrology (cont'd.)

[Contact: Joseph R. Kinard, (301) 975-4250]

Kinard, J.R., Lipe, T.E., and Childers, C.B., **AC-DC Difference Relationships for Current Shunt and Thermal Converter Combinations**, Digest of the 1990 Conference on Precision Electromagnetic Measurements, Ottawa, Canada, June 11-14, 1990, pp. 136-137 (1990).

This paper describes the relationship between the overall ac-dc difference of a thermal converter and current shunt combination and the characteristics of the separate thermal converter and current shunt. As a consequence of the analysis, an expression predicting the ac-dc difference of a thermal converter/shunt combination when thermoelements are interchanged is presented, and data illustrating the agreement between values of ac-dc difference and values predicted by the analysis are given.

[Contact: Joseph R. Kinard, (301) 975-4250]

Oldham, N.M., and Henderson, R.M., **New Low-Voltage Standards in the DC to 1 MHz Frequency Range**, Digest of the 1990 Conference on Precision Electromagnetic Measurements, Ottawa, Canada, June 11-14, 1990, pp. 66-67 (1990).

Several new techniques for measuring the rms value of 1- to 200-mV signals have been developed and compared to existing techniques using thermal transfer standards. Differences between the various measurement methods at 100 mV are typically within  $\pm 100$  parts per million from dc to 1 MHz.

[Contact: Nile M. Oldham, (301) 975-2408]

Steiner, R.L., and Astalos, R.J., **Improvements for Automating Voltage Calibrations Using a 10-V Josephson Array**, Digest of the 1990 Conference on Precision Electromagnetic Measurements, Ottawa, Canada, June 11-14, 1990, pp. 102-103 (1990).

With three novel improvements, a voltage standard system based on a 10-V Josephson array is totally automated. A commercial standard cell scanner controls switching for calibrating either Zener references or digital voltmeters, a programmable attenuator helps in obtaining voltage steps, and measurements of DVM noise help in verifying array stability.

[Contact: Richard Steiner, (301) 975-4226]

Fundamental Electrical Measurements

## Released for Publication

Cage, M.E., Yu, D., Jeckelmann, B.M., Steiner, R.L., and Duncan, R.V., **Investigating the Use of Multimeters to Measure Quantized Hall Resistance Standards**.

A new generation of digital multimeters was used to directly compare the ratios of the resistances of wire-wound reference resistors and quantized Hall resistances. The accuracies are better than 0.1 ppm for ratios as large as 4:1 if the multimeters are calibrated with a Josephson array.

[Contact: Marvin E. Cage, (301) 975-4249]

## Recently Published

Olsen, P.T., Tew, W.L., Elmquist, R.E., and Williams, E.R., **Monitoring the Mass Standard: A Comparison of Mechanical to Electrical Power**, Digest of the 1990 Conference on Precision Electromagnetic Measurements, Ottawa, Canada, June 11-14, 1990, pp. 180-181 (1990).

Except for the kilogram, all of the base units of the International System of Units (SI) are defined by invariant fundamental constants. The on-going NIST absolute watt experiment shows the promise of being able to monitor the stability of the mass standard to better than 0.05 ppm. We discuss our latest results and future possibilities.

[Contact: P. Thomas Olsen, (301) 975-6553]

Cryoelectronic Metrology

Released for Publication

Beall, J.A., Cromar, M.W., Harvey, T.E., Johansson, M.E., Ono, R.H., Reintsema, C.D., Rudman, D.A., Nelson, A.J., Asher, S.E., and Swartzlander, A.B., **YBa<sub>2</sub>Cu<sub>3</sub>O<sub>x</sub>/Insulator Multi-Layers for Crossover Fabrication.**

The development of thin-film dielectrics compatible with epitaxial growth of YBa<sub>2</sub>Cu<sub>3</sub>O<sub>x</sub> (YBCO) is crucial to the fabrication of multilayer device and circuit structures. We have investigated the SrTiO<sub>3</sub>, (STO)/YBCO system by fabricating YBCO/STO bilayers and simple YBCO/STO/YBCO 'crossover' structures. The thin films were deposited in situ by pulsed laser deposition and analyzed using X-ray diffraction and scanning electron microscopy. The film interfaces were characterized by secondary-ion-mass spectroscopy depth profiling. We have developed photolithographic and wet etching processes for patterning the crossovers which are compatible with these materials. The crossover structures were characterized by resistance and insulator pinhole density, as well as the superconducting properties of the patterned top and bottom YBCO electrodes (critical temperature, critical current density ( $J_c$ )). Using SrTiO<sub>3</sub> as the insulating layer, we have made crossovers with good isolation between layers (>100 MΩ) and high  $J_c$  even in the top electrode ( $J_c(76\text{ K} > 10^5\text{ A/cm}^2)$ ).

[Contact: James A. Beall, (303) 497-5989]

Grossman, E.N., McDonald, D.G., and Sauvageau, J.E., **Far-Infrared Kinetic Inductance Detector**, to be published in IEEE Transactions on Magnetics (Proceedings of 1990 Applied Superconductivity Conference, Snowmass, Colorado, September 24-28, 1990).

Extremely sensitive far-infrared detectors suitable for both direct detection and heterodyne applications are possible based on micrometer-sized thin films with

thickness less than a superconducting penetration depth. The penetration depth of such a film, and therefore its inductance, varies with temperature and with quasiparticle population (described by an effective temperature  $T^*$ ), resulting in both bolometric and nonequilibrium "photoinductive" responses. Incident radiation is coupled into the small-area kinetic inductor via a lithographic antenna, and the resulting inductance changes are amplified and converted to a voltage signal by an integrated microstrip dc SQUID. The device is sensitive because, unlike junction-based devices with large capacitive reactances, the kinetic inductor is naturally well matched to the antenna impedance at the far-IR frequency and to the pre-amplifier (SQUID) impedance at IF or video frequencies. The best kinetic inductor materials are those with low electronic mean free path, large penetration depth, and high critical-current density. Thus, common magnet alloys such as NbTi are the natural choice for liquid-He temperature operation. A detailed analysis predicts a (phonon-limited) noise equivalent power of about  $4 \times 10^{-17}\text{ W/Hz}^{1/2}$  for a bolometer with an iridium kinetic inductor operated at 0.1 K. A heterodyne noise temperature of 2250 K at 3 THz, with 200-MHz bandwidth is predicted for a NbTi mixer operated at 4 K.

[Contact: Erich N. Grossman, (303) 497-5102]

Park, G.S., Cunningham, C.E., Cabrera, B., and Huber, M.E., **Study of Trapped Vortices in a Superconducting Microbridge**, to be published in IEEE Transactions on Magnetics (Proceedings of 1990 Applied Superconductivity Conference, Snowmass, Colorado, September 24-28, 1990).

We are experimenting with optical switches for use in a noise-reduction device for SQUID magnetometers. Laser light pulsed onto an Nb microbridge drives it momentarily normal and changes the quantum flux state of a superconducting circuit. For certain laser pulse parameters, a vortex is sometimes

Cryoelectronic Metrology (cont'd.)

trapped in the microbridge and is detected by a SQUID coupled to the circuit. The trapping frequency and vortex position were studied using various waveforms.

[Contact: Martin E. Huber, (303) 497-5423]

Przybysz, J., Miller, D., and Hamilton, C.A., **Josephson Counting Analog-to-Digital Converter**, to be published in IEEE Transactions on Magnetics (Proceedings of 1990 Applied Superconductivity Conference, Snowmass, Colorado, September 24-28, 1990).

A superconductive analog-to-digital converter that uses a dc SQUID quantizer and a flip-flop counter has been designed, fabricated, and tested. The circuit was fabricated using a ten-level niobium process. Tests at 4.2 K demonstrated (1) counting to the full 12-bit accuracy of the design, and (2) monotonic A/D conversion with linearity to 1 LSB over the nearly eight-bit range allowed by the test equipment.

[Contact: Clark A. Hamilton, (303) 497-3840]

Sauvageau, J.E., McDonald, D.G., and Grossman, E.N., **Superconducting Kinetic Inductance Bolometer**, to be published in IEEE Transactions on Magnetics (Proceedings of 1990 Applied Superconductivity Conference, Snowmass, Colorado, September 24-28, 1990).

We are developing a bolometer based on a differential thermometer that senses temperature changes through changes in the kinetic inductance of a superconducting thin film. The temperature transducer is an inductance bridge patterned as an integrated circuit on a 1-cm<sup>2</sup> Si substrate. Two inductors from opposite arms of the bridge are patterned on a thermally-isolated Si island, 2 mm<sup>2</sup>, which is supported by a 9- $\mu$ m thick Si:B membrane. The bridge is excited with audio frequency current, and the bridge imbalance is detected using a commercial

dc SQUID amplifier. The bridge is balanced by applying power to the thermally isolated island. The thermometer is coupled to an IR absorbing cone by a thermal link consisting of fine Cu braid. The composite bolometer is the sensor for a prototype radiometer that will provide an absolute measure of IR power. The radiometer, which is designed for an NEP of about  $10^{-11}$  W/ $\sqrt{\text{Hz}}$ , is intended to measure the spectrally dispersed power of a 300-K black body. This absolute radiometer is being developed for use at the Low Background Infrared (LBIR) Facility at the National Institute of Standards and Technology, Gaithersburg, Maryland. The noise floor of the temperature transducer for the radiometer has been measured to be 0.75 pW for a 100-s integration time. This is 150 times lower noise level than that of the commercial absolute radiometer currently used at the LBIR Facility in Gaithersburg.

[Contact: Joseph E. Sauvageau, (303) 497-3770]

## Recently Published

Hamilton, C.A., Burroughs, C.J., and Chieh, K., **Operation of NIST Josephson Array Voltage Standards** [original title: Operation of Josephson-Array Voltage Standards], Journal of Research of the National Institute of Standards and Technology, Vol. 95, No. 3, pp. 219-235 (May-June 1990).

This paper begins with a brief discussion of the physical principles and history of Josephson voltage standards. The main body of the paper deals with the practical details of the array design, cryoprobe construction, bias source requirements, adjustment of the system for optimum performance, calibration algorithms, and an assessment of error sources.

[Contact: Clark A. Hamilton, (303) 497-3740]

Martinis, J.M., and Ono, R.H., **Fabrication of Ultrasmall Nb-AlO<sub>x</sub>-Nb Josephson Tunnel Junctions**, Applied Physics Let-

Cryoelectronic Metrology (cont'd.)

ters, Vol. 57, No. 6, pp. 629-631 (6 August 1990).

We describe a fabrication process to make Nb-AlO<sub>x</sub>-Nb edge junctions with areas down to 0.0022 μm<sup>2</sup> and with current densities from 10 to 24000 A/cm<sup>2</sup>. The junction conductance was low for voltages below the superconducting energy gap, indicating good quality tunnel barriers. Coulomb gap measurements obtained when the junctions were in the normal state were used to find the junction capacitance. Junction capacitance as small as 0.18 fF has been measured.

[Contact: John M. Martinis, (303) 497-3597]

Pulse Power Metrology

## Recently Published

FitzPatrick, G.J., Olthoff, J.K., Simmon, E.D., and Fenimore, Jr., C.P., **Metrology for Space Power: Metrology Development and Survey of Space-Based Measurements**, NISTIR 4422 (September 1990).

This report documents technical progress in the three investigations comprising the project "SDI Measurement Techniques" funded by the Strategic Defense Initiative Office. The first investigation assesses the applicability of magneto-optic sensors for measuring submicrosecond-risetime current pulses. The results of comparative measurements with fiber optic current sensors and conventional detectors are reported. The optical sensors have sufficient bandwidth, but sensor stability is a problem, especially for remote applications. The second investigation develops part of the mathematical background needed for assessing the reliability and efficiency of diagnostics used in the development and deployment of pulsed power components and systems. Through comparative measurements, characteristic signatures of nonlinearities in an electro-optic voltage measurement system of the order of 1% in magnitude have been detected.

Nonlinearities in a conventional detector have been investigated through appropriate models. The third investigation involves the accumulation of existing information necessary to support an effective measurement development program. The results of an in-depth study of existing space-based measurement techniques are reported, and the findings indicate that present space-based measurement systems are inadequate for anticipated SDI requirements.

[Contact: Gerald J. FitzPatrick, (301) 975-2737]

Antenna Metrology

## Recently Published

Hill, D.A., **Electric and Magnetic Dipole Radiation in a Random Medium**, *Electromagnetics*, Vol. 10, pp. 279-292 (1990). (Previously published as Sections 4 and 5 of NISTIR 89-3909.)

Electric and magnetic dipole radiation are studied for a medium where random, small-scale inhomogeneities are confined to a spherical shell region. Numerical results are presented for both the far-field pattern and the total radiated power. When the random inhomogeneities are located in the near field of the source, an electric dipole radiates a larger incoherent field than a magnetic dipole because of its larger reactive electric field.

[Contact: David A. Hill, (303) 497-3472]

Microwave & Millimeter-Wave Metrology

## Recently Published

Kinard, J.R., Huang, D.X., and Novotny, D.B., **Hybrid Construction of Multijunction Thermal Converters**, Digest of the 1990 Conference on Precision Electromagnetic Measurements, Ottawa, Canada, June 11-14, 1990, pp. 62-63 (1990).

Using thin-film and thick-film technologies, multijunction thermal converters have been designed for fre-

Microwave & Millimeter-Wave (cont'd.)

quencies ranging from audio up to tens of megahertz and for heater currents from a few milliamperes up to hundreds of milliamperes. This paper describes these designs and the early production of prototype converters.

[Contact: Joseph R. Kinard, (301) 975-4250]

Kinard, J.R., Huang, D.X., and Rebuldela, G., **RF-DC Differences of Thermal Voltage Converters Arising from Input Connectors**, Digest of the 1990 Conference on Precision Electromagnetic Measurements, Ottawa, Canada, June 11-14, 1990, pp. 280-281 (1990).

The radiofrequency-dc differences of thermal voltage converters caused by skin effect and transmission line effects of different length input structures have been previously studied. Discrepancies do exist, however, between simple mathematical models and measured results for commonly used input connectors. This paper reports a study of these discrepancies.

[Contact: Joseph R. Kinard, (301) 975-4250]

Optical Fiber Metrology

Released for Publication

Gilbert, S.L., **Frequency Stabilization of a Tunable Erbium-Doped Fiber Laser**. [Summary paper on the same topic (Frequency Stabilization of an Erbium-Doped Fiber Laser: A Potential Wavelength Standard for Optical Communications) will be given at the Conference on Optical Fiber Communications, San Diego, California, February 18-22, 1991.]

A single-frequency erbium-doped fiber laser has been constructed which is tunable from 1520 nm to 1580 nm. The laser linewidth was determined to be less than 1.6 MHz full width half maximum by observing the spectrum of the beat between the fiber laser and a 1523-nm helium-neon laser. The frequency of the

fiber laser was locked to several absorption lines of acetylene near 1530 nm. This work demonstrates the inherent stability of fiber lasers and evaluates their potential for use in a wavelength standard for optical communications.

[Contact: Sarah L. Gilbert, (303) 497-3120]

## Recently Published

Day, G.W., and Franzen, D.L., (Editors), **Technical Digest -- Symposium on Optical Fiber Measurements, 1990**, NIST Special Publication 792 (September 1990).

This digest contains summaries of 46 papers presented at the Symposium on Optical Fiber Measurements, held September 11-12, 1990, at the National Institute of Standards and Technology, Boulder, Colorado. Paper titles: Industry standard measurements: a user's perspective; COST 217 interlaboratory comparison of optical measurements on single-mode fiber couplers; COST 217 mode field diameter measurements intercomparison; Post-mortem analysis of optical fibers; Optical frequency domain reflectometry using network analysis techniques; Long and short range measurements using coherent frequency-modulated, continuous-wave reflectometry; Very low optical return loss measurement using optical time-domain reflectometry technique; Comparison between optical time-domain reflectometry and optical low-coherence reflectometry (OLCR) with micrometer spatial resolution: new improved OLCR detection scheme and latest measurement results on IOC; Multiphoton pulse approach in photon-timing optical time-domain reflectometry yields enhanced dynamic range and shorter measurement time; Characterization of hydrogen diffusion in hermetically coated optical fibers; The anomalous structure observed in single-mode fiber cutoff wavelength measurements: theory and solutions; A recent advance in the measurement of the refractive index profile of optical fiber preforms; Refractive index measurements on single-mode fiber as functions of product parameters, tensile stress and

Optical Fiber Metrology (cont'd.)

temperature; Spatially resolved measurement of high attenuation in integrated optical polarizers; Waveguide loss and effective indices determination by optical frequency scan of integrated resonant cavities.

Measurement of mode indices of channel waveguides by interferometry; Comparison of time and frequency domain measurement methods for high speed optical modulators; Characterization of the dynamic response of a waveguide phase modulator by means of an optical frequency discriminator; Fiber discriminator measurements of phase modulation in an integrated Mach-Zehnder intensity modulator; Characterization of erbium-doped fiber amplifiers; Measurement of the spectral dependence of absorption cross section for erbium-doped single-mode optical fiber; Wavelength characterization of components for optical networking applications in the 1.5- $\mu\text{m}$  transmission window; Measurement of laser diode intensity noise below the shot noise limit; An optical synthesizer with sinusoidal-modulated Michelson interferometer for generation of an absolutely stabilized carrier frequency comb; Characterization of high birefringence fiber for sensor applications; Interpretation of polarization dispersion in a single-mode fiber; Polarization mode dispersion of short and long single-mode fibers; Distributed strain measurements in optical fibers using Brillouin optical-fiber time domain analysis; Standards for optical fiber geometry measurements; A comparison of interferometric techniques for fiber cladding diameter measurements.

Accurate determination of cladding diameter and noncircularity of optical fibers; Calibration of fiber diameter measurements; Fiber geometry measurement and quality of parameter estimation; Pulse-delay measurement for long zero-dispersion fibers; Measurement of reduced germania (GeO) defect levels in optical fibers by fluorescence and absorption

spectroscopy; Standardized measurement for determining the radiation-induced attenuation in optical fibers; Test method for fiber optic connector parameters directly affecting return loss Differentiating core and cladding loss contributions in single mode fiber attenuation measurements; A single launch technique to determine loss and dispersion in multimode fiber systems; Measurement of fiber coating geometry using transversely scanning laser beam; Reliability testing of a fiber optic system for subscriber loop applications; Accurate modal characterization of passive components based on selective excitation of optical fibers; The modulation transfer function for coupling components; Loss reflectance, in-line, continuously variable attenuator for lightwave system characterization; and Photorefractive intermodal exchangers (PRIME) in optical fiber: theory and applications.

[Contact: Gordon W. Day, (303) 497 5204]

Optical Fiber Sensors

Released for Publication

Deeter, M.N., Rose, A.H., and Day, G.W. **Faraday-Effect Magnetic Field Sensor Based on Substituted Iron Garnets**, to be published in the Proceedings of SPIE (The International Society for Optical Engineering, P.O. Box 10, Bellingham Washington 98227-0010), Fiber Optic and Laser Sensors VIII, San Jose, California, September 16-21, 1990.

The performance of fiber-optic magnetic field sensors based on the Faraday effect mainly depends on the magneto-optical properties of the sensor element. Certain ferrimagnetic materials known as substituted iron garnets display characteristics which make them suitable for applications of magnetometry requiring high sensitivity, high spatial resolution, or high speed. The potential of these materials for magnetic field sensing is illustrated by comparing results of measurements made on two different iron garnet compositions.

Optical Fiber Sensors (cont'd.)

[Contact: Merritt Deeter, (303) 497-5400]

Deeter, M.N., Rose, A.H., and Day, G.W., **Iron-Garnet Magnetic Field Sensors with 100 pT/ $\sqrt{\text{Hz}}$  Noise-Equivalent Field**, to be published in the Conference Digest, Seventh International Conference on Optical Fiber Sensors, Sydney, Australia, December 3-6, 1990.

The sensitivity of Faraday-effect sensors incorporating diamagnetically-substituted yttrium iron garnet (YIG) is potentially much higher than of sensors employing pure YIG. Results of Faraday rotation linearity and sensitivity measurements are presented for gallium-substituted YIG. At 500 Hz, the noise-equivalent magnetic field is approximately 100 pT/ $\sqrt{\text{Hz}}$ .

[Contact: Merritt N. Deeter, (303) 497-5400]

Tang, D., Rose, A.H., and Day, G.W., **Optical Fiber Current Sensors with Temperature Stabilities Near the Material Limit**, to be published in the Conference Digest, Seventh International Conference on Optical Fiber Sensors, Sydney, Australia, December 3-6, 1990.

We describe an optical fiber current sensor with a normalized temperature coefficient of  $+8.4 \times 10^{-5}/\text{K}$  over the range from  $-75$  to  $+145$  °C. This is within 20% of the limit set by the temperature dependence of the Verdet constant measured in bulk silica. Packaging of the sensor degrades its stability, but a fully packaged coil with a stability of  $+1.7 \times 10^{-4}/\text{K}$  over the range from  $-30$  to  $+125$  °C has also been demonstrated.

[Contact: Allen H. Rose, (303) 497-5599]

Veesser, L.R., and Day, G.W., **Faraday Effect Current Sensing Using a Sagnac Interferometer with a 3x3 Coupler**, to be published in the Conference Digest, Seventh International Conference on

Optical Fiber Sensors, Sydney, Australia, December 3-6, 1990.

We demonstrate a fiber optic current sensor based on a Sagnac interferometer with a 3x3 sensor. Compared to the more common Sagnac with a 2x2 coupler, this design offers the additional benefits of a greater response for small signals and the unambiguous interpretation of signals that exceed the period of the response function.

[Contact: Gordon W. Day, (303) 497-5204]

Williams, P.A., Rose, A.H., Day, G.W., and Deeter, M.N., **Temperature Dependence of the Verdet Constant in Several Diamagnetic Glasses.**

We report measurements of the temperature dependence of the Verdet constant of SiO<sub>2</sub>, SF-57, and BK-7 glasses. In each case, the Verdet constant increases with temperature by the order of 1 part in 10<sup>4</sup>/K over the range from room temperature to 150 °C. The results for each glass are within 3 to 20% of estimates obtained using the Becquerel formula with published data for dispersion and the change in index of refraction with temperature.

[Contact: Paul A. Williams, (303) 497-3287]

#### Recently Published

FitzPatrick, G.J., Olthoff, J.K., Simmon, E.D., and Fenimore, Jr., C.P., **Metrology for Space Power: Metrology Development and Survey of Space-Based Measurements**, NISTIR 4422 (September 1990).

This report documents technical progress in the three investigations comprising the project "SDI Measurement Techniques" funded by the Strategic Defense Initiative Office. The first investigation assesses the applicability of magneto-optic sensors for measuring submicrosecond-risetime current pulses. The results of comparative measurements with fiber optic current sensors and conventional detectors are reported. The

Optical Fiber Sensors (cont'd.)

optical sensors have sufficient bandwidth, but sensor stability is a problem, especially for remote applications. The second investigation develops part of the mathematical background needed for assessing the reliability and efficiency of diagnostics used in the development and deployment of pulsed power components and systems. Through comparative measurements, characteristic signatures of nonlinearities in an electro-optic voltage measurement system of the order of 1% in magnitude have been detected. Nonlinearities in a conventional detector have been investigated through appropriate models. The third investigation involves the accumulation of existing information necessary to support an effective measurement development program. The results of an in-depth study of existing space-based measurement techniques are reported, and the findings indicate that present space-based measurement systems are inadequate for anticipated SDI requirements.

[Contact: Gerald J. FitzPatrick, (301) 975-2737]

Electro-Optic Metrology

Released for Publication

Sanford, N.A., Malone, K.J., and Larson, D.R., **Integrated-Optic Waveguide Glass Lasers**, to be published in the Digest of the Conference on Optical Fiber Communications, San Diego, California, February 18-22, 1991.

Rare-earth-doped integrated-optic waveguide devices offer new miniaturized cw and pulsed lasers, amplifiers, and other active elements. Fabrication methods which use bulk glasses, as well as chemical-vapor deposition techniques, are being explored.

[Contact: Norman A. Sanford, (303) 497-5239]

Sanford, N.A., Malone, K.J., and Larson, D.R., **Mode-Locked and Q-Switched Operation of Extended-Cavity Integrated-**

Optic Lasers.

Integrated-optic lasers operating near 1057 nm have been actively mode-locked and Q-switched in an extended-cavity fashion. The waveguide structures were made by electric-field-assisted ion exchange in neodymium-doped soda-lime silicate glass. CW pumping was accomplished with a Ti:sapphire laser. The repetition rate of the mode-locked pulses was 100 MHz. A minimum mode-locked pulse width of approximately 80 ps full width at half maximum was measured; the peak power was 182 mW. Q-switched operation of a similar device using a 57-cm-long cavity configuration produced 75-ns full width at half maximum pulses with peak powers of 1.2 W.

[Contact: Norman A. Sanford, (303) 497-5239]

Veasey, D.L., Hickernell, R.K., Larson, D.R., and Batchman, T.E., **Waveguide Polarizers Using Hydrogenated Amorphous Silicon Claddings.**

We have fabricated TE- and TM-pass waveguide polarizers with polarization extinction ratios of 42 and 35 dB respectively. The devices were fabricated by the growth of hydrogenated amorphous silicon claddings on  $K^+Na^+$  ion exchanged channel waveguides in glass. Cladding thicknesses were accurately tuned to permit optimum coupling of either a TE or TM mode to the cladding. We have also demonstrated that waveguide losses of at least 760 dB/cm can be measured using a photothermal deflection technique.

[Contact: David L. Veasey, (303) 497-3439]

Recently Published

Larson, D.R., and Phelan, Jr., R.J., **Hydrogenated Amorphous Germanium Detectors Deposited onto Channel Waveguides**, Optics Letters, Vol. 15, No. 10, pp 544-546 (May 15, 1990).

We have fabricated hydrogenated amorphous germanium photodetectors coupled to

Electro-Optic Metrology (cont'd.)

channel waveguides in glass and lithium niobate substrates. We measured a pulse response duration of 140 psec (full width at half maximum), which is shorter than that of any previously reported photo-detectors deposited onto dielectric waveguides. The optical gap, which determines the spectral response characteristics, is approximately 1.2 eV. We have measured a photoconductive gain of 18 in phosphorus-doped detectors.

[Contact: Donald R. Larson, (303) 497-3440]

Electromagnetic Properties

## Released for Publication

van Roggen, A., Yuwono, L., Zhou, H., Meijer, P.H.E., and Kopanski, J.J., **Permittivity Measurements on Molecular-Sized Samples**, to be published as an Extended Abstract, will be presented as poster only at the IEEE Conference on Electrical Insulation and Dielectric Phenomena (CEIDP), Pocono Manor, Pennsylvania, October 29-November 1, 1990.

A new laboratory on Molecular Electronics has been started at the Physics Department of the Catholic University of America. In our efforts to make organic bistable devices, one of the research functions of this laboratory is to measure the electrical properties of materials and active devices made with molecular (mainly organic) materials. The size of material samples, and the specimens used for measurement, is exceedingly small, typically layers with a thickness of the order of 100 nm. Consequently, the setups used for normal dielectric and conductivity measurements ( $\geq 10$ -mm electrode size) cannot be used, and special cells and instrumentation have to be developed.

[Contact: Joseph J. Kopanski, (301) 975-2089]

Other Fast Signal Topics

## Released for Publication

Capobianco, T.E., and Ciciora, S.J., **Characterizing Differential Air-Core Eddy Current Probes**, to be published in the Proceedings of the Review of Progress in Quantitative Nondestructive Evaluation Conference, La Jolla, California, September 15-20, 1990.

We report the results of measurements establishing the flaw response of a differential, air-core, eddy current probe. The parameters chosen for the probe's construction were picked from a set of 32 combinations of five factors which were varied at two levels. These five factors include: (1) the number of layers of the inner coils, (2) the number of layers of the outer coil, (3) the number of turns on the inner coils, (4) the number of turns on the outer coil, and (5) the inside diameter of the inner coils. We report the results of calibrating this probe constructed in our laboratory, and we also discuss some of the idiosyncracies we encountered in the calibration process. The calibration reported here was carried out on seven notches made by electrical discharge machining in blocks of 7075-T6 aluminum alloy. The probe output is correlated to changes in flaw area.

[Contact: Thomas E. Capobianco, (303) 497-3141]

Danielson, B.L., and Boisrobert, C.Y., **Absolute Optical Ranging Using Low Coherence Interferometry**.

We describe a method for measuring submicrometer distances with an asymmetric fiber Michelson interferometer having an LED as a source of radiation. By measuring the phase slope of the Fourier components in the frequency domain, it is possible to locate the position of reflections with nanometer precision even in the presence of sample dispersion. The method is compatible with time-domain sampling at the Nyquist rate which ensures efficiency in data acquisition and processing.

[Contact: Bruce L. Danielson, (303) 497-5620]

Other Fast Signal Topics (cont'd.)

Obarski, G., and Young, M., **Transverse Aberration of Glass Plates.**

We derive an exact expression for the transverse aberration of a tilted plate. For moderate thicknesses, the beam remains diffraction limited only if F-number  $\geq 11$ .

[Contact: Gregory Obarski, (303) 497-5747]

## Recently Published

Bell, B.A., Perrey, A.G., and Treado, M.J., **Evaluation of Hands-Free Communication Systems**, NISTIR 90-4230 (August 1990).

Hands-Free Communication Systems (HFCS) are used by law enforcement agencies, fire departments, rescue squads, and the Armed Forces, where tasks require the communications operator's hands to be free. Four such HFCSs were tested to measure their operational characteristics of voltage gain/frequency response, signal-to-noise ratio, total harmonic distortion, and sensitivity.

[Contact: Barry A. Bell, (301) 975-2402]

Capobianco, T.E., **Eddy Current Probe Characterization Using an Impedance Plane Display Instrument** [original title: Using an Eddy Current Impedance Plane Display Instrument for Probe Characterization], Proceedings of the 38th Defense Conference on Non-destructive Testing (NDT), San Antonio, Texas, October 31-November 2, 1989, pp. 193-201 (1990).

The U.S. Army is sponsoring work at the National Institute of Standards and Technology to develop a military standard for characterizing the performance of eddy-current probes for nondestructive testing. Presently, the test method of this draft standard constitutes a measurement of the change in probe impedance when the probe is applied to test blocks of two different conductivities.

It was hoped that this impedance measurement would be easy to perform in the field, but we discovered that field and depot level operations lack the equipment for measuring impedance, a serious obstacle to the implementation of the standard. However, depot operations often have an eddy-current instrument which displays flaw signals in the impedance plane. These instruments do not display the actual impedance values for the flaw signals, but could possibly be calibrated for this purpose. Results are presented of an experiment where a calibration technique was tried and eddy-current probe impedances measured. The calibration technique consists of using a switchable combination of resistors and inductors to produce reference points on the display of the impedance-plane instrument. The impedance measurements were made by interpolating values from these reference points for flaw signals obtained when the probes were scanned over an electrical discharge machined notch in 6061-T651 aluminum.

[Contact: Thomas E. Capobianco, (303) 497-3141]

Fulcomer, P.M., **Prospects for the Use of Lithium Batteries in Law Enforcement Equipment**, National Institute of Justice Technology Assessment Report, NIJ Report 201-89 (April 1990).

Lithium batteries have been available for a number of years, mainly in primary type (nonrechargeable), low-current-drain configurations (i.e., less than 10 mA). Within the past several years, more medium-to-high-current drain (50- to 500-mA) lithium primary cells have become available, and within the past few years lithium secondary cells (rechargeable) have been introduced. The advantages of lithium include better low-temperature performance and much longer shelf life for primary cells, and superior charge retention and lack of a memory effect for secondary cells. Both types can provide significantly more power per volume and per weight than equivalent nonlithium batteries. In addition to the advantages and disadvantages of lithium batteries

Other Fast Signal Topics (cont'd.)

and their applicability for use in law enforcement equipment, this report discusses lithium battery background, the safety precautions required in the use of lithium cells, and the battery requirements for present law enforcement equipment. The report concludes that the use of lithium batteries would be beneficial to the operation of most battery-operated equipment used by law enforcement personnel. To fully realize the advantages mentioned above, however, and to minimize the effect of their higher initial cost, lithium batteries should, with two exceptions, be designed into new equipment.

[Contact: P. Michael Fulcomer, (301) 975-2407]

## ELECTRICAL SYSTEMS

Power Systems Metrology

Released for Publication

Olthoff, J.K., Van Brunt, R.J., Heron, J.T., and Sauers, I., **Sensitive Detection of Trace  $S_2F_{10}$  in  $SF_6$ .**

A new method is described for detection of  $S_2F_{10}$  in  $SF_6$  down to the part-per-billion level. The method utilizes a gas chromatograph-mass spectrometer (GC/MS) equipped with a jet separator and a heated gas inlet tube connected to the electron-impact ionizer of the MS. The  $S_2F_{10}$  is converted to  $SO_2$  in the heated stainless-steel inlet tube at temperatures above 150 °C by a surface catalyzed reaction involving  $H_2O$ . As a consequence of this conversion, peaks corresponding to  $S_2F_{10}$  appear on single-ion chromatograms at ion masses characteristic of  $SO_2$  ( $m/z = 48, 67, \text{ and } 86$ ) where there is little or no interference from  $SF_6$  features. By this method, a direct analysis of  $SF_6$  for  $S_2F_{10}$  content can be performed in a relatively short time since the enrichment procedure previously required for GC/MS methods can be eliminated. Problems associated with the preparation and maintenance of reliable,

stable  $S_2F_{10}$  reference samples are discussed.

[Contact: James K. Olthoff, (301) 975-2431]

Olthoff, J.K., Van Brunt, R.J., Wang, H-X., Moore, J.H., and Tossell, J.A., **Absolute Total Electron Scattering and Dissociative Attachment Cross Sections of By-Products from Electrical Discharges in  $SF_6$ ,** to be published in the Proceedings of the Sixth International Symposium on Gaseous Dielectrics, Knoxville, Tennessee, September 23-27, 1990.

Using an electron transmission spectrometer, the absolute total dissociative attachment cross sections of  $SF_6$  and of its decomposition products have been measured as a function of electron energy over the range of 0.2 eV to 5.0 eV, and absolute total electron scattering cross sections have been measured from 0.2 eV to 12 eV. These results are presented along with previous data where available. [Contact: James K. Olthoff, (301) 975-2431]

Sauers, I., Harman, G., Olthoff, J.K., and Van Brunt, R.J.,  **$S_2F_{10}$  Formation by Electrical Discharges in  $SF_6$ : Comparison of Spark and Corona,** to be published in the Proceedings of the Sixth International Symposium on Gaseous Dielectrics, Knoxville, Tennessee, September 23-27, 1990.

Among the  $SF_6$  by-products of electrical discharges that have been investigated,  $S_2F_{10}$  is probably the least understood (physical, chemical, and biological properties) and the most toxic. Its production in electrical discharges has been controversial since the presence of this chemical has been reported by only a few groups. We report on the yields of  $S_2F_{10}$  in two types of discharges: spark and corona. The  $S_2F_{10}$  yields for corona and spark were 2.4  $\mu\text{mol/C}$  and 0.04 to 0.37  $\text{nmol/J}$ , respectively, for experiments where the water content was low. For both types of discharges, we have found that  $S_2F_{10}$  formation is dependent on the presence of moisture. For corona

Power Systems Metrology (cont'd.)

discharges, model calculations based on known sulfur-fluorine chemistry are shown to yield reasonable agreement with experimental data. We show that  $S_2F_{10}$  was formed in electrical discharges expected to be found in compressed-gas insulated equipment, and address such factors as effects of moisture and surface conditions.

[Contact: James K. Olthoff, (301) 975-2425]

Stricklett, K.L., Van Brunt, R.J., and Steiner, J.P., **Recent Advances in Partial Discharge Measurement Capabilities at NIST**, to be published in the Proceedings of the 1990 International Workshop on Methods for Partial Discharge Measurement and Their Traceability, Villa Olmo, Italy, September 4-6, 1990.

An advanced real-time partial discharge (PD) measurement system is described which allows a "complete" characterization of the stochastic properties of partial discharges. With this system it is possible to measure a set of conditional PD pulse-amplitude and pulse-time-separation distributions from which memory effects characteristic of the discharge phenomena can be quantified and interpreted. Examples of results obtained for negative pulsating discharges in gases are shown. Results obtained from fast photographic studies of PDs in liquid dielectrics are discussed. The methods employed allow simultaneous determinations of the current waveform and a photographic record of the discharge growth in a liquid dielectric. These data provide a detailed description of the temporal and spatial development of a PD at its inception. A time-domain reflectometry technique is also described which allows location of PD pulses in cables.

[Contact: Kenneth L. Stricklett, (301) 975-3955]

Van Brunt, R.J., and Kulkarni, S., **Influence of Memory on the Statistics of Pulsating Corona**, to be published in the

Proceedings of the Sixth International Symposium on Gaseous Dielectrics, Knoxville, Tennessee, September 23-27, 1990.

In order to develop a theory that accounts for observed pulse-time separation and pulse-amplitude distributions for pulsating corona discharges in gases, it is necessary to consider the effects of residuals from prior discharge pulses, such as ion space charge and metastables, on the development of subsequent pulses. Such "memory effects" are shown here to be significant in controlling the statistics of Trichel-pulse corona in electro-negative gases. The memory effects are quantitatively assessed from a direct measurement of a set of conditional pulse-amplitude and pulse-time-separation distributions. The effectiveness of this method in providing a more complete description and better understanding of the stochastic behavior of corona is illustrated here for the case of self-sustained Trichel pulse in a neon-oxygen gas mixture. The amplitude and time of initiation of any discharge pulse is found to be strongly dependent on the amplitude of the previous pulse, as well as on the time that has elapsed since that pulse occurred. Memory is found to extend back beyond the most recent pulse so that the process is distinctly non-Markovian.

[Contact: Richard J. Van Brunt, (301) 975-2425]

Van Brunt, R.J., Kulkarni, S.V., and Lakdawala, V., **Transition from Trichel-Pulse Corona to Dielectric Barrier Discharge**, to be published in the 1990 Annual Report of the Conference on Electrical Insulation and Dielectric Phenomena, Pocono Manor, Pennsylvania, October 29-31, 1990.

Experiments are conducted to investigate the conditions under which the transition from negative corona to dielectric barrier-controlled discharge occurs. A negative point-plane electrode (covered with polytetrafluoroethylene dielectric) geometry is studied using a newly developed partial discharge detection tech-

Power Systems Metrology (cont'd.)

nique. At a critical gap distance, an abrupt transition from a rapid pulsating behavior to a widely distributed random pulse behavior is observed. The critical distance increases with increasing diameter of the solid dielectric and decreases with increase in applied voltage. The influence of dielectric surface charging on the Trichel pulse behavior is manifested by the measured pulse-height and time-separation distributions. As the influence of dielectric charging increases, the pulse separation distribution begins to broaden significantly, and the corresponding pulse-height distribution becomes narrower. The previously observed strong correlation between pulse height and time separation from the previous pulse is also persistent under all conditions of experimentation. The expected behavior can be attributed to the perturbation of applied field at the tip of the cathode due to surface charging of the solid dielectric. Once the Trichel-pulse behavior ceases, the rate of discharge pulsation becomes controlled by the rate of the surface charge dissipation on the dielectric.

[Contact: Richard J. Van Brunt, (301) 975-2425]

## Recently Published

Fenimore, C., Stricklett, K.L., Yamashita, H., Kawai, H., Forster, E.O., and Pompili, M., **The Inception and Structure of Prebreakdown Streamers in Perfluorinated Polyethers**, Conference Record of the Tenth International Conference on Conduction and Breakdown in Dielectric Liquids, Grenoble, France, September 10-14, 1990, pp. 430-435 (September 1990).

One member of a family of materials, the perfluorinated polyethers, is subjected to electrical measurements to determine its suitability as a liquid dielectric. Measures of the breakdown strength and streamer inception voltage are obtained under electrical impulse stress. The breakdown strength is nearly independent

of polarity. Under high magnification photography, the cathode-originated streamers are seen to have a subsonic mode of growth. The transition to fast growth occurs on time and spatial scales shorter than those reported in liquid hydrocarbons. The gas phase electrical properties and the high heat of vaporization of this material are considered as mechanisms for this behavior.

[Contact: Charles Fenimore, (301) 975-2428]

Filipski, P.S., Moore, W.J.M., Knight, R.B.D., Martin, P., and Oldham, N.M., **An International Comparison of Low Audio Frequency Power Meter Calibrations Conducted in 1989**, Digest of the 1990 Conference on Precision Electromagnetic Measurements, Ottawa, Canada, June 11-14, 1990, pp. 158-159 (1990).

The results of an intercomparison of low-audio-frequency power meter calibrations conducted in 1989 between the National Research Council (NRC), Canada, the National Physical Laboratory (NPL), United Kingdom, and the National Institute of Standards and Technology (NIST), USA, are described. A time-division watt-converter, developed at NRC, was used as the transfer standard. The measurements were made at 120 V, 5 A, power factors of 1, 0 lead, and 0 lag and at frequencies up to 5 kHz. Agreement between the NPL and NRC laboratories was better than 63 ppm in the 60- to 1600-Hz range, and 74 ppm between NIST and NRC in the 50- to 4800-Hz range.

[Contact: Nile M. Oldham, (301) 975-2408]

Oldham, N.M., Laug, O.B., Waltrip, B.C., and Palm, R.H., **The NIST Digitally Synthesized Power Calibration Source**, NIST Technical Note 1281 (August 1990).

A digitally synthesized source of "phantom" power for calibrating electrical power and energy meters is described. Independent sources of voltage, current, and phase angle are programmable between 0 to 240 V, 0 to 5 A, and 0 to 360 deg, respectively. The uncertainty of the

Power Systems Metrology (cont'd.)

active and reactive power is estimated to be within  $\pm 100$  ppm of the full-scale apparent power (volt-amperes).

[Contact: Nile M. Oldham, (301) 975-2408]

Ramboz, J.D., Fenimore, C., and Schiller, S.B., **Qualifying Watthour Meters for Use as MAP Transport Standards**, Digest of the 1990 Conference on Precision Electromagnetic Measurements, Ottawa, Canada, June 11-14, 1990, pp. 329-330 (1990).

The NIST Measurement Assurance Program (MAP) transfers the watthour using transport meters. A statistical design is employed to determine the linear and nonlinear corrections for the response of each meter to varying conditions of voltage, current, temperature, and power factor. For applications requiring lower precision, a heuristic for dropping correction terms is given.

[Contact: John D. Ramboz, (301) 975-2434]

Ramboz, J.D., and West, J.L., **Watt Transfer Standard**, Digest of the 1990 Conference on Precision Electromagnetic Measurements, Ottawa, Canada, June 11-14, 1990, pp. 160-161 (1990).

The use of a time-division multiplier power meter as a watt transfer standard between the National Institute of Standards and Technology (NIST) and an industry standards laboratory is described. Measurements of power at 120 and 240 V, 5 A, 50 and 62 Hz, and power factors of 1 and 0 lagging are described. After the unit of power was transferred to the industrial laboratory, a comparison of the laboratory and NIST calibrations indicated an agreement to within 14 parts per million.

[Contact: John D. Ramboz, (301) 975-2434]

Stricklett, K.L., Kelley, E.F., Yamashita, H., Fenimore, C., Pace, M.O., Blalock, T.V., Wintenburg, A.L., and

Alexeff, I., **Observations of Partial Discharges in Hexane Under High Magnification**, Conference Record of the Tenth International Conference on Conduction and Breakdown in Dielectric Liquids, Grenoble, France, September 10-14, 1990, pp. 381-386 (September 1990).

Partial discharges are observed in hexane by shadow photography under the application of dc voltages. A nonuniform field geometry is employed, and the growth of low-density streamers at a point cathode is recorded. Photographs of the partial discharge streamers are obtained at 200X magnification. The use of an image-preserving optical delay allows a record of the conditions which exist in the liquid prior to the initiation of the low-density streamer to be obtained. A concurrent record of the partial discharge current is obtained. Analysis of these data indicates that electrostatic forces are adequate to describe streamer growth.

[Contact: Kenneth L. Stricklett, (301) 975-3955]

Yamashita, H., Kawai, H., Stricklett, K.L., and Kelley, E.F., **The Effect of High Pressure on Prebreakdown Phenomena in N-Hexane**, Conference Record of the Tenth International Conference on Conduction and Breakdown in Dielectric Liquids, Grenoble, France, September 10-14, 1990, pp. 404-409 (September 1990).

The effect of pressure on the initiation of prebreakdown streamers at a point cathode in n-hexane is investigated. Using a high-magnification (100X) high-resolution (1- $\mu\text{m}$ ) optical system and a high-speed camera, the initial growth of low-density streamers at pressures ranging from 0.1 to 1.1 MPa is examined. The initial streamer appears to be a single filament  $4.1 \pm 2.1 \mu\text{m}$  in length. The streamer initiation voltage is shown to increase with pressure and the rate of collapse of the streamer is faster at high pressure.

[Contact: Hisanao Yamashita, (301) 975-5826]

Superconductors

Released for Publication

Beall, J.A., Cromar, M.W., Harvey, T.E., Johansson, M.E., Ono, R.H., Reintsema, C.D., Rudman, D.A., Nelson, A.J., Asher, S.E., and Swartzlander, A.B., **YBa<sub>2</sub>Cu<sub>3</sub>O<sub>x</sub>/Insulator Multi-Layers for Crossover Fabrication.**

The development of thin-film dielectrics compatible with epitaxial growth of YBa<sub>2</sub>Cu<sub>3</sub>O<sub>x</sub> (YBCO) is crucial to the fabrication of multilayer device and circuit structures. We have investigated the SrTiO<sub>3</sub>, (STO)/YBCO system by fabricating YBCO/STO bilayers and simple YBCO/STO/YBCO 'crossover' structures. The thin films were deposited in situ by pulsed laser deposition and analyzed using X-ray diffraction and scanning electron microscopy. The film interfaces were characterized by secondary-ion-mass spectroscopy depth profiling. We have developed photolithographic and wet etching processes for patterning the crossovers which are compatible with these materials. The crossover structures were characterized by resistance and insulator pinhole density, as well as the superconducting properties of the patterned top and bottom YBCO electrodes (critical temperature, critical current density ( $J_c$ )). Using SrTiO<sub>3</sub> as the insulating layer, we have made crossovers with good isolation between layers (>100 M $\Omega$ ) and high  $J_c$  even in the top electrode ( $J_c(76\text{ K}) > 10^5\text{ A/cm}^2$ ).

[Contact: James A. Beall, (303) 497-5989]

Cross, R.W., and Goldfarb, R.B., **Enhanced Flux Creep in Nb-Ti Superconductors After an Increase in Temperature.**

The magnetic fields of superconducting-super-collider (SSC) dipole magnets are known to change with time when the magnets are operated at constant current. The decay of the field is thought to be a consequence of flux creep in the Nb-Ti filaments in the superconducting cables. However, measured magnetic relaxation of

small samples of SSC cable as a function of time is unlike the large decays with long time constants that are observed in the fields of the actual magnets. We have made relaxation measurements on sample SSC conductors at 3.5 and 4.0 K after field cycling. The decay at both temperatures was 1.8% in 30 min. However, the relaxation measured after a temperature increase from 3.5 to 4.0 K was 4.9% in 30 min. A likely reason for the greater magnetization decay is that, after an increase in temperature, the Nb-Ti is in a supercritical state, with shielding currents flowing at a density greater than the new critical current density. This causes enhanced flux creep. We suggest that a small temperature rise during the operation of SSC magnets may be responsible for the unexpectedly large magnetic field decay. [Contact: R. William Cross, (303) 497-5300]

Cross, R.W., and Goldfarb, R.B., **Hall Probe Magnetometer for SSC Magnet Cables: Effect of Transport Current on Magnetization and Flux Creep.**

We constructed a Hall probe magnetometer to measure the magnetization hysteresis loops of superconducting-super-collider magnet cables. The instrument uses two Hall-effect field sensors to measure the applied field  $H$  and the magnetic induction  $B$ . Magnetization  $M$  is calculated from the difference of the two quantities. The Hall probes are centered coaxially in the bore of a superconducting solenoid with the  $B$  probe against the sample's broad surface. An alternative probe arrangement, in which  $M$  is measured directly, is with the sample probe parallel to the field. We measured  $M$  as a function of  $H$  and cycle rate both with and without a dc transport current. Flux creep as a function current was measured from the dependence of ac loss on the cycling rate and from the decay of magnetization with time.

[Contact: R. William Cross, (303) 497-5300]

Ekin, J.W., and Bray, S.L., **Effect of**

Superconductors (cont'd.)**Transverse Stress on the Critical Current of Bronze-Process and Internal-Tin Nb<sub>3</sub>Sn.**

The effect of transverse stress on the measured critical current of two substantially different Nb<sub>3</sub>Sn superconductors, a bronze-process conductor and an internal-tin conductor, has been measured. Photomicrographs of the two conductors reveal a basic difference in their microstructure. The bronze-process conductor exhibits columnar grains that are radially oriented within the Nb<sub>3</sub>Sn filaments, while the grains of the internal-tin conductor are more equiaxed and randomly oriented. The radial orientation of the bronze-process grains defines an anisotropy between the axial and transverse directions that might account for the greater sensitivity of the critical current to transverse stress reported previously. The effect of transverse stress on the internal-tin conductor, however, is comparable to that of the bronze-process conductor. Thus, these data indicate that the transverse stress effect is not highly dependent on either grain morphology or fabrication process. From an engineering standpoint, the similarity of the transverse stress effect for these two types of Nb<sub>3</sub>Sn superconductors represents an important simplification for setting first-order quantitative limits on the mechanical design of large superconducting magnets. [Contact: John W. Ekin, (303) 497-5448]

**Goodrich, L.F., High-T<sub>c</sub> Superconductor Voltage-Current Simulator and the Pulse Method of Measuring Critical Current.**

A passive voltage-current (V-I) simulator has been developed and tested using pulse-current and conventional direct-current methods. The simulator was designed to generate the extremely nonlinear V-I characteristic of a superconductor. It is intended to be used to test various components of the measurement system such as instrumentation, measurement method, and data analysis

software to determine the transport critical current or critical current density of a superconductor. Since this simulator does not emulate all of the subtle effects of a superconductor, it provides a necessary but not sufficient test of the measurement system. A comparison of preliminary results of the pulse-current and direct-current methods on the passive simulator are presented. Also, comparisons of methods using bulk and thin-film YBCO samples are given. [Contact: Loren F. Goodrich, (303) 497-3143]

**Goodrich, L.F., Moreland, J., and Roshko A., Switching in High-T<sub>c</sub> Superconductor Current Transport Measurements.**

Switching voltages can occur in four wire current transport measurements on sintered high-T<sub>c</sub> superconductors. These switching voltages are irreversible shifts in the voltage-current characteristic of the superconductor that result in multiple branches of the voltage-current characteristic. The voltage along these branches can be very nonlinear with respect to current and can be positive or negative in polarity relative to the current direction. These voltages can interfere with the correct determination of resistivity and critical current density. Experimental data on non-aligned sintered high-T<sub>c</sub> material are presented which illustrate the complex nature of the voltages and the confusion they can create. Models based on weak links and H<sub>c1</sub>, and other effects are discussed along with observations on conventional (low T<sub>c</sub>) superconductors. [Contact: Loren F. Goodrich, (303) 497-3143]

**Goodrich, L.F., and Srivastava, A.N. Software Techniques to Improve Data Reliability in Superconductor and Low Resistance Measurements.**

The software techniques described here have been used in a variety of measurements, such as resistance-versus-temperature measurements made on cryoconductors or superconductors, and voltage versus

Superconductors (cont'd.)

current measurements made on superconductors to determine the critical current. These techniques have been developed to take low-amplitude data in various patterns, assign a figure of merit to a set of data readings, edit data for erroneous reading (or other experimental variations), and to alert the experimenter if the detected errors are beyond the scope of the software. Erroneous voltage readings from digital voltmeters, intermittent electrical connections, and an array of similar variations in data has been detected through the use of data editors. Two data editors have been developed: the fixed-limit editor and the dynamic editor. These editors remove readings that are inconsistent with the distribution of the majority of the data readings. The frequency of erroneous readings from a particular digital voltmeter range from 1 error per 100,000 readings to 1 error per 100 readings. The magnitude of the error can be as large as 60 V with a 0-V input to the voltmeter. A systematic study was performed on the occurrence of the internally generated erroneous voltmeter readings, and it was determined that the amount that a reading was in error scaled with one of a few parameters.

[Contact: Loren F. Goodrich, (303) 497-1143]

Moreland, J., and Rice, P., **Tunneling Stabilized Magnetic Force Microscopy: Prospects for Low Temperature Applications to Superconductors**, to be published in IEEE Transactions on Magnetics (Proceedings of 1990 Applied Superconductivity Conference, Snowmass, Colorado, September 24-28, 1990).

We have recently demonstrated an imaging technique referred to as tunneling stabilized magnetic force microscopy (TSMFM). TSMFM is performed using a scanning tunneling microscope (STM) with a flexible, magnetic, tunneling tip in place of the usual rigid tunneling tip. TSMFM images are therefore combinations of topography and the magnetic forces

between the tip and the sample. Room-temperature TSMFM images of bit tracks on a hard disk have 100-nm resolution and are comparable to Bitter patterns made using a ferrofluid. We are presently building a low-temperature STM for TSMFM of the flux lattice in superconductors. Design and testing of the apparatus are discussed along with preliminary results. [Contact: John Moreland, (303) 497-3641]

Ono, R.H., Beall, J.A., Harvey, T.E., Reintsema, C.D., Johansson, M., Cromar, M.W., Goodrich, L.F., Moreland, J., and Roshko, A., **Critical Current Behavior of Ag-Diffused  $\text{YBa}_2\text{Cu}_3\text{O}_{7-\delta}$  Thin Films**.

We have studied the behavior of high-quality  $\text{YBa}_2\text{Cu}_3\text{O}_{7-\delta}$  (YBCO) thin films with Ag over-layers. In some cases, the Ag was diffused into the high- $T_c$  film post-annealing. We chose to study Ag in detail because of its widespread use as contact metallization and our earlier studies of proximity effects in YBCO. The details of transport critical-current measurements are presented. The Ag coatings can reduce normal state resistance while not degrading  $J_c$ .

[Contact: Ronald H. Ono, (303) 497-3762]

Ono, R.H., Goodrich, L.F., Beall, J.A., Johansson, M.E., and Reintsema, C.D., **Magnetic Field Dependence of the Critical Current Anisotropy in Normal Metal- $\text{YBa}_2\text{Cu}_3\text{O}_{7-\delta}$  Thin Film Bilayers**.

We have measured the transport critical current density ( $J_c$ ) in epitaxial-quality films of  $\text{YBaCu}_3\text{O}_{7-\delta}$  which were covered by thin (10-nm) Ag films. The films, both with and without Ag, had  $J_c$  values greater than 10 A/cm in liquid nitrogen. The effect of the Ag was to greatly reduce the dependence of  $J_c$  on external magnetic fields, but only in the case where the field was oriented in the plane of the film perpendicular to the c axis. It is unlikely that the effect is simply due to altered surface pinning, although qualitative agreement with critical state models is observed.

Superconductors (cont'd.)

[Contact: Ronald H. Ono, (303) 497-3762]

Petersen, T.W., and Goldfarb, R.B., **Effect of Mechanical Deformation on Nb-Ti Filament Proximity-Effect Coupling at the Edges of SSC Cables.**

Magnetization as functions of transverse magnetic field and time was measured for short strands extracted from the centers and edges of five Nb-Ti Rutherford cables designed for use in superconducting-super-collider dipole magnets. The strands all had 6- $\mu\text{m}$  diameter filaments. Edge samples, which had severe mechanical deformation, showed small magnetic coupling losses at low fields, compared to no coupling losses for undeformed center strands. This suggests that the cabling process decreases the interfilament spacing to the order of the coherence length in the normal matrix material, resulting in an increase in effective filament diameter and hysteresis loss at low fields. Microscopic studies of the cables' cross sections confirmed smaller interfilament separations in these samples. Flux creep measurements, represented by the time dependence of magnetization, showed little difference between edge and center samples. This indicates that the proximity-coupled matrix in edge samples is not a significant source of flux creep. [Contact: Timothy W. Petersen, (303) 497-5333]

Russek, S.E., Jeanneret, B., and Ekin, J.W., **Properties of  $\text{YBa}_2\text{Cu}_3\text{O}_{7-\delta}$  Thin Films Grown on Off-Axis-Cut MgO Substrates.**

A series of  $\text{YBa}_2\text{Cu}_3\text{O}_{7-\delta}$  films has been reactively sputtered on off-axis-cut MgO substrates. It was found that all the films were oriented with the c-axis normal to the substrate regardless of substrate orientation, indicating that growth dynamics is a major factor influencing film orientation on non-lattice matched substrates. As the

substrate orientation is moved off the (100) direction, the films showed a decrease in transition temperature and showed properties indicative of an increased density of weak links. On high-angle substrates, the films showed improved properties over the films on low-angle substrates. Films grown on (110) MgO were as good as films grown on (100) MgO.

[Contact: Steven E. Russek, (303) 497-5097]

Walsh, T., Moreland, J. Ono, R.H., Beall, J.A., Cromar, M.W., Harvey, T., Reintsema, C., and Kalkur, T.S., **Tunneling Spectroscopy of High Critical Temperature Superconductors Using Squeezable Electron Tunneling Junctions.**

We have performed tunneling spectroscopy measurements on squeezable electron tunneling (SET) junctions using Bi-Sr-Ca-Cu-O, Y-Ba-Cu-O, and Nb electrodes in a variety of combinations. A zero-bias conductance peak has been seen repeatedly in the current-voltage [I(V)] and conductance-voltage [G(V)] characteristics. We present a model to explain this conductance peak in terms of quasi-particle tunneling, phase diffusion, and a supercurrent. Two additional structures have been seen repeatedly in I(V) and G(V). One of these structures has the characteristics of an energy gap feature. The other structure, which can mimic the gap feature, is explained in terms of the switching to the voltage state of a grain boundary junction that is in series with the SET junction. The dependence of these features upon temperature and the force applied to the junction is examined.

[Contact: Thomas Walsh, (303) 497-5430]

Walsh, T., Moreland, J., Ono, R.H., and Kalkur, T.S., **Tunneling Measurements of the Zero-Bias Conductance Peak and the Bi-Sr-Ca-Cu-O Thin Film Energy Gap.**

We have used squeezable electron tunneling junctions, at 4 K, to examine the zero-bias conductance peak that has been found in high-temperature superconductors.

Superconductors (cont'd.)

unnel junction spectra by a number of researchers. In addition, peaks in the differential conductance-voltage characteristic have been found repeatedly between 46 and 64 mV. We interpret the voltages at which these peaks occur to be the gap voltage, denoted  $2\Delta(4\text{ K})$ . The zero-bias conductance peak can be explained in terms of a supercurrent and thermal excitations, both quasi-particles and phase diffusion.

Contact: Thomas Walsh, (303) 497-5430]

## Recently Published

Bray, S.L., and Goodrich, L.F., **Current Supply for High- $T_c$  Superconductor Testing** [original title: High- $T_c$  Current Supply for DC Critical-Current Measurements], Measurement Science Technology, Vol. 1, pp. 491-494 (1990).

Precise and accurate measurements of the critical current of high  $T_c$  superconductors often require a current supply that has high stability and low output ripple. A design for a simple and inexpensive current supply that has these characteristics is presented. The primary power source for this supply is a 12-V wet-cell battery. The typical operating range of the current supply is from 10 mA to 10 A. The performance of the supply with respect to current ripple, stability, and linearity is reported.

Contact: Steven L. Bray, (303) 497-31]

Williams, E.W., Marken, Jr., K.R., Sumption, M.D., Goldfarb, R.B., and Doughran, R.J., **AC Loss Measurements of Two Multifilamentary NbTi Composite Strands**, Advances in Cryogenic Engineering (Materials), Vol. 36, pp. 169-176 (1990).

As part of an interlaboratory comparative testing program conducted in support of the Versailles Agreement on Advanced Materials and Standards (VAMAS), transverse-field dc hysteresis loss measure-

ments were made at liquid-helium temperatures at fields of up to 3 T (30 kG) on two samples of multifilamentary NbTi composite. The strands differed widely in filament number, were comparable in filament diameter, and one of them was provided with a Cu-Ni barrier between the filaments. The results have been analyzed, and magnetically deduced critical current density values obtained (for comparison with directly measured transport data) using various standard techniques. Based on these studies, a figure-of-merit for ac loss is recommended. The Cu-matrix strand, with its interfilamentary spacing of less than  $1\ \mu\text{m}$ , exhibited pronounced proximity-effect-induced coupling losses; this was not observed in the mixed-matrix strand which possessed not only a Cu-Ni barrier but also an interfilamentary spacing of typically  $4\ \mu\text{m}$ .

[Contact: Ronald B. Goldfarb, (303) 497-3650]

Ekin, J.W., Hart, Jr., H.R., and Gadipati, A.R., **Transport Critical Current of Aligned Polycrystalline  $Y_1Ba_2Cu_3O_{7-\delta}$  and Evidence for a Nonweak-Linked Component of Intergranular Current Conduction**, J. Appl. Phys., Vol. 68, No. 5, pp. 2285-2295 (1 September 1990).

A study of grain alignment and its effect on the dc transport critical current in fine-grained bulk  $Y_1Ba_2Cu_3O_{7-\delta}$  is reported in magnetic fields from  $10^{-4}$  T to 26 T. Two features distinguish the critical-current density  $J_c$  of aligned bulk  $Y_1Ba_2Cu_3O_{7-\delta}$  from unaligned material. First, the effective critical field where the intergranular  $J_c$  approaches zero is about four times higher (30 T) for aligned samples with field parallel to the a, b planes, than it is for polycrystalline unaligned samples (7 T). Second, the nearly field-independent plateau value of  $J_c$  between 10 mT and 1 T is one to two orders of magnitude higher than typical plateau values of  $J_c$  in unaligned bulk-sintered  $Y_1Ba_2Cu_3O_{7-\delta}$ , for field parallel to the a, b planes. A low-field (<10-mT) weak-link decrease in  $J_c$  with magnetic field is still observed,

Superconductors (cont'd.)

but it is much smaller than for unaligned material. These data clearly demonstrate that alignment alone significantly reduces the weak-link problem in fine-grained polycrystalline samples with low-aspect-ratio (4:1) grains (unlike melt-grown samples where there has been some ambiguity as to the relative importance of alignment versus large grain growth). Furthermore, the results provide strong evidence that there are two parallel components of intergranular current conduction, one consisting of weak-linked material, the other behaving like intrinsic intragranular material that is not weak-linked. A comparison with unaligned  $Y_1Ba_2Cu_3O_{7-\delta}$  indicates that the volume fraction of such nonweak-linked material is significantly enhanced by grain alignment, but still only 0.01% to 0.1% of the grain boundary area. Field-cooled and force-free  $J_c$  data are also presented, along with detailed measurements of the shapes of the voltage-current characteristics.

[Contact: John W. Ekin, (303) 497-5448]

Goldfarb, R.B., and Ishida, T., **Fundamental and Harmonic Susceptibilities of  $YBa_2Cu_3O_{7-\delta}$** , Physical Review B, Vol. 41, No. 13, pp. 8937-8948 (1 May 1990).

We have examined the complex harmonic magnetic susceptibilities  $\chi_n = \chi_n' - i\chi_n''$  ( $n = 1, 2, 3, \dots, 10$ ) of the sintered high-critical-temperature superconductor  $YBa_2Cu_3O_{7-\delta}$  (YBCO). The experimental variables for the measurements of  $\chi_n$  were the sample temperature ( $10 \leq T \leq 110$  K), the ac magnetic field amplitude  $H_{ac}$  ( $1.4 \mu T \leq \mu_0 H_{ac} \leq 8.5$  mT) and frequency  $f$  ( $7.3 \leq f \leq 1460$  Hz), and the magnitude of a superimposed dc field  $H_{dc}$  ( $0 \leq \mu_0 H_{dc} \leq 8.5$  mT). As functions of temperature,  $\chi_1'$  and  $\chi_1''$  depend on both  $H_{ac}$  and  $H_{dc}$ . In particular, the  $\chi_1'$  transition curve may shift to higher temperatures with increasing  $H_{dc}$ . Odd-harmonic susceptibilities were measured as functions of temperature below  $T_c$  for zero  $H_{dc}$ ; both even and odd harmonics were observed for nonzero  $H_{dc}$ . The temperature dependence

of  $\chi_3$  is a strong function of  $H_{ac}$ .  $|\chi_3|$  has a maximum below the critical temperature  $T_c$ , similar to the peak in  $\chi_1''$ , which is slightly frequency dependent. At a fixed temperature, the odd-harmonic susceptibilities are even functions of  $H_{ac}$ , while the even-harmonic susceptibilities are odd functions of  $H_{ac}$ . We compared the experimental intergrain coupling characteristics of  $\chi_n'$  and  $\chi_n''$  with theoretical susceptibility curves based on magnetization equations derived by Ji et al. from a simplified Kim model for critical current density. The theoretical curves are in good agreement with the temperature- and field-dependent features of  $\chi_n'$  and  $\chi_n''$ , and thus, the intergrain coupling component of a sintered high- $T_c$  superconductor has the properties of a type-I superconductor.

[Contact: Ronald B. Goldfarb, (303) 497-3650]

Goldfarb, R.B., and Spomer, R.L., **Magnetic Characteristics and Measurements of Filamentary Nb-Ti Wire for the Superconducting Super Collider**, Advances in Cryogenic Engineering (Materials), Vol. 36, pp. 215-222 (1990).

In synchrotron accelerator applications, such as the superconducting super collider (SSC), superconducting magnets are cycled in magnetic field. Desirable properties of the magnets include field uniformity, field stability with time, small residual field, and fairly small energy losses upon cycling. This paper discusses potential sources of problems in achieving these goals, describes important magnetic characteristics to be considered, and reviews measurement techniques for magnetic evaluation of candidate SSC wires. Instrumentation that might be practical for use in a wide fabrication environment is described. We report on magnetic measurements of prototype SSC wires and cables and speculate on causes for instability in multipole fields of dipole magnets constructed with such cables.

[Contact: Ronald B. Goldfarb, (303) 497-3650]

Superconductors (cont'd.)

Goodrich, L.F., and Bray, S.L., **High- $T_c$  Superconductors and the Critical Current Measurement**, Cryogenics, Vol. 30, pp. 667-677 (August 1990).

With the introduction of high- $T_c$  superconductors, a number of problems associated with the critical-current ( $I_c$ ) measurement has arisen. The existing  $I_c$  measurement practices have been developed and proven for low- $T_c$  superconductors. There are substantial differences between the two classes of materials. When the concept was casually extended to the high- $T_c$  conductors, the problems of measurement inconsistency, ambiguity, and in some cases, invalidity followed. A discussion of the underlying philosophy of the  $I_c$  measurement is presented. Also, a number of measurement variables that can influence the measured  $I_c$  are discussed. Many of the problems stem from inadequate  $I_c$  reporting practices. Recommendations are given for improving measurement reports.

[Contact: Loren F. Goodrich, (303) 497-143]

Man, Z., Budnick, J.I., Bouldin, C.E., Jojicik, J.C., Cheong, S-W., Cooper, A.S., Espinosa, G.P., and Fisk, Z., **Polarization X-ray Absorption Near-Edge Structure Study of  $Pr_{2-x}Ce_xCuO_4$  Single Crystals: The Nature of Ce Doping**, Physical Review B, Vol. 42, No. 1, pp. 1037-1040 (1 July 1990).

polarization Cu K-edge x-ray absorption near-edge structure (XANES) study has been carried out on  $Pr_{2-x}Ce_xCuO_4$  single crystals. The spectra for X-ray polarization vector  $E$  nearly parallel to the crystal c-axis suggest that electrons contributed by Ce doping are initially localized at the Cu site. The spectra for  $E$  perpendicular to the c-axis exhibit almost rigid edge shift to lower energy upon Ce doping. This suggests that at the unoccupied in-plane Cu 4p states shift to lower energies. Therefore, the doping donates electrons to the Cu site and also shifts the unoccupied 4p

band. We propose that the upper unoccupied band consisting of predominately Cu 3d states shifts downward and eventually joins the initially localized states near the Fermi level and thus, forms the conduction band in the n-type superconductor.

[Contact: Charles E. Bouldin, (301) 975-2046]

Magnetic Materials & Measurements

## Released for Publication

Cross, R.W., and Goldfarb, R.B., **Hall Probe Magnetometer for SSC Magnet Cables: Effect of Transport Current on Magnetization and Flux Creep**.

We constructed a Hall probe magnetometer to measure the magnetization hysteresis loops of superconducting-super-collider magnet cables. The instrument uses two Hall-effect field sensors to measure the applied field  $H$  and the magnetic induction  $B$ . Magnetization  $M$  is calculated from the difference of the two quantities. The Hall probes are centered coaxially in the bore of a superconducting solenoid with the  $B$  probe against the sample's broad surface. An alternative probe arrangement, in which  $M$  is measured directly, is with the sample probe parallel to the field. We measured  $M$  as a function of  $H$  and cycle rate both with and without a dc transport current. Flux creep as a function current was measured from the dependence of ac loss on the cycling rate and from the decay of magnetization with time.

[Contact: R. William Cross, (303) 497-5300]

Deeter, M.N., Rose, A.H., and Day, G.W., **Faraday-Effect Magnetic Field Sensors Based on Substituted Iron Garnets**, to be published in the Proceedings of SPIE (The International Society for Optical Engineering, P.O. Box 10, Bellingham, Washington 98227-0010), Fiber Optic and Laser Sensors VIII, San Jose, California, September 16-21, 1990.

The performance of fiber-optic magnetic

Magnetic Materials & Meas. (cont'd.)

field sensors based on the Faraday effect mainly depends on the magneto-optic properties of the sensor element. Certain ferrimagnetic materials known as substituted iron garnets display characteristics which make them suitable for applications of magnetometry requiring high sensitivity, high spatial resolution, or high speed. The potential of these materials for magnetic field sensing is illustrated by comparing results of measurements made on two different iron garnet compositions. [Contact: Merritt Deeter, (303) 497-5400]

Deeter, M.N., Rose, A.H., and Day, G.W., **Iron-Garnet Magnetic Field Sensors with 100 pT/ $\sqrt{\text{Hz}}$  Noise-Equivalent Field**, to be published in the Conference Digest, Seventh International Conference on Optical Fiber Sensors, Sydney, Australia, December 3-6, 1990.

The sensitivity of Faraday-effect sensors incorporating diamagnetically-substituted yttrium iron garnet (YIG) is potentially much higher than of sensors employing pure YIG. Results of Faraday rotation linearity and sensitivity measurements are presented for gallium-substituted YIG. At 500 Hz, the noise-equivalent magnetic field is approximately 100 pT/ $\sqrt{\text{Hz}}$ . [Contact: Merritt N. Deeter, (303) 497-5400]

Goldfarb, R.B., and Chen, D-X., **Demagnetizing Factors for Cylinders**.

We have calculated fluxmetric and magnetometric demagnetizing factors  $N_f$  and  $N_m$  for cylinders as functions of susceptibility  $\chi$  and the ratio of length to diameter  $\gamma$ . For  $\chi = 0$ , applicable to weakly magnetic or saturated ferromagnetic materials,  $N_f$  and  $N_m$  are calculated using a formula for the mutual inductance of concentric coaxial thin solenoids.  $N_f$  for  $-1 \leq \chi < \infty$  and  $N_m$  for  $\chi \rightarrow \infty$  when  $\gamma \geq 10$  are calculated using a one-dimensional model. For  $1 \leq \gamma \leq 10$ , an important

range for magnetometer measurements,  $N_m$  for both  $\chi \rightarrow \infty$  and  $\chi < 0$  are obtained by extrapolation from data at larger  $\gamma$ . The case  $\chi < 0$  is applicable to conductors and superconductors. General rules for demagnetizing factors are discussed. [Contact: Ronald B. Goldfarb, (303) 497-3650]

Rice, P., and Moreland, J., **A New Look at the Bitter Method of Magnetic Imaging**.

A scanning-tunneling microscope (STM) was used in place of an optical microscope in the Bitter method to image the magnetic ferrofluid particles on the surface of a hard disk. The Bitter method is a reliable method to look at magnetic patterns on magnetic storage media. The resolution obtainable is limited by the optical viewing of the magnetic particles. Using the scanning tunneling microscope, we have obtained image resolution limited only by the ferrofluid particle size and the sharpness of the STM tip. [Contact: Paul Rice, (303) 497-3841]

## Recently Published

Goldberg, I.B., Mitchell, M.R., Murphy, A.R., Goldfarb, R.B., and Loughran, R.J., **Magnetic Susceptibility of Inconel Alloys 718, 625, and 600 at Cryogenic Temperatures**, Advances in Cryogenic Engineering (Materials), Vol. 36, pp 755-762 (1990).

In June 1988, the Discovery Space Shuttle mission was delayed because of a malfunctioning hydrogen fuel bleed valve system. The problem was traced to the linear variable differential transformer (LVDT) which produced erroneous readings for the valve position. Near liquid hydrogen temperatures, the inconel used in the armature of the LVDT became magnetic. The alternating current magnetic susceptibility of three samples of inconel 718, that differed slightly in composition, and one sample of inconel 625 were measured as a function of temperature. Inconel 718 behaves as a spin glass. Its susceptibility reaches a maximum between 15 and 19 K, near the

Magnetic Materials & Meas. (cont'd.)

liquid hydrogen boiling point, 20 K. The magnitude of the susceptibility changed by an order of magnitude with decreases of 1.2% in iron and 1.5% in nickel. The nominal composition is 12 to 20% iron and 0 to 55% nickel. Inconel 625, which contains about 4% iron, was paramagnetic. The qualitative behavior of these materials follows trends indicated by Chauvenard (1928) and Jackson and Russell (1938).

Contact: Ronald B. Goldfarb, (303) 497-6550]

Moreland, J., and Rice, P., High-Resolution Tunneling-Stabilized Magnetic Imaging and Recording, Applied Physics Letters, Vol. 57, No. 3, pp. 310-312 (16 July 1990).

A scanning tunneling microscope (STM) has been used to image and record magnetic regions on the surface of a computer hard disk. The usual rigid STM tip was replaced by a compliant magnetized Fe film tip. As a result, tunneling images were combinations of the surface topography and variations in the magnetic force between the Fe film tip and the disk surface. We believe that the recording process relied on maintaining the close proximity of a magnetized Fe film tip near the disk surface. Apparently, the magnetic field was focused near the film tip with sufficient intensity to change the surface magnetization of the disk. We have recorded spots on the disk within a 500 by 500 nm<sup>2</sup> area. These spots were subsequently imaged with the same STM tip. Our best magnetic image resolution was 20 nm. The compliance of the Fe film tips was such that image contrast due to variation of the magnetic force on the Fe film tip corresponded to motion piezoelectric elongations as large as 50 nm.

Contact: John Moreland, (303) 497-3641]

Peterson, R.L., Magnetization of Anisotropic Superconducting Grains, Journal of Applied Physics, Vol. 67, No. 11, pp. 6930-6933 (1 June 1990).

A critical-state calculation of the magnetization of hard type-II superconducting grains having anisotropic critical-current densities is given. The grains are assumed to present rectangular cross sections to an applied magnetic field. The analysis shows how the critical-current densities should be inferred from magnetization measurements for various grain dimensions. For grains in the form of platelets, the hysteresis changes with grain size. However, for very elongated grains with anisotropic critical currents, such as may be found in the high-temperature superconductors, the magnetic hysteresis is insensitive to the lengths of the grains, and hence to powdering.

[Contact: Robert L. Peterson, (303) 497-3750]

Other Electrical Systems Topics

## Released for Publication

Fickett, F.R., The Roles of Copper in Applied Superconductivity, to be published in the Proceedings of the CU90 Conference, Vasteras, Sweden, October 1-4, 1990.

Copper plays many roles in applied superconductivity, but its contribution is seldom acknowledged. In low-temperature superconductors, it serves as a stabilizer, protecting the cable or wire against destruction in the event of a quench. In addition, the stabilizing copper, with suitable additions of other elements, can act to magnetically decouple the superconductor filaments in fine-filament conductors. In large magnets, such as those used in high-energy physics and fusion-energy experiments, large pieces of cold copper are often used as thermal transfer sections. Less commonly, copper alloys are sometimes used as a structural material in place of the more usual stainless steel. In some experimental configurations, copper is used to shield against rapidly changing magnetic and electromagnetic fields. Most of the high-temperature ceramic superconductors are based on copper oxide, and there is some possibility that

Other Electrical Systems Topics (cont'd.)

at least some of these ceramics will be compatible with a copper stabilizer in the (future) applications of these materials. In this paper, we review the uses of copper in each of the categories mentioned above, both historically and in the latest applications. A brief description of the desired properties of the copper used for each application is given, along with some suggestions as to how to achieve these properties in commercial copper products.

[Contact: Fred R. Fickett, (303) 497-3785]

## ELECTROMAGNETIC INTERFERENCE

Radiated Electromagnetic Interference

## Recently Published

Hill, D.A., **Electric and Magnetic Dipole Radiation in a Random Medium**, *Electromagnetics*, Vol. 10, pp. 279-292 (1990). (Previously published as Sections 4 and 5 of NISTIR 89-3909.)

Electric and magnetic dipole radiation are studied for a medium where random, small-scale inhomogeneities are confined to a spherical shell region. Numerical results are presented for both the far-field pattern and the total radiated power. When the random inhomogeneities are located in the near field of the source, an electric dipole radiates a larger incoherent field than a magnetic dipole because of its larger reactive electric field.

[Contact: David A. Hill, (303) 497-3472]

## ADDITIONAL INFORMATION

Lists of Publications

Lyons, R.M., and Gibson, K.A., **A Bibliography of the NIST Electromagnetic Fields Division Publications**, NISTIR 3945 (August 1990).

This bibliography lists publications by the staff of the National Institute of

Standards and Technology's Electromagnetic Fields Division for the period from January 1970 through August 1989. Selected earlier publications from the Division's predecessor organizations are included.

[Contact: Kathryn A. Gibson, (303) 497-3132]

DeWeese, M.E., **Metrology for Electromagnetic Technology: A Bibliography of NIST Publications**, NISTIR 89-3921 (August 1989).

This bibliography lists the publications of the personnel of the Electromagnetic Technology Division of NIST in the period from January 1970 through publication of this report. A few earlier references that are directly related to the present work of the Division are included.

[Contact: Sarabeth Moynihan, (303) 497-3678]

Palla, J.C., and Meiselman, B., **Electrical and Electronic Metrology: A Bibliography of NIST Electricity Division's Publications**, NIST List of Publications 94 (January 1990).

This bibliography covers publications of the Electricity Division, Center for Electronics and Electrical Engineering, NIST, and of its predecessor sections for the period January 1968 to December 1989. A brief description of the Division's technical program is given in the introduction.

[Contact: Jenny C. Palla, (301) 975-2220]

Walters, E.J., **Semiconductor Measurement Technology**, NBS List of Publications 72 [a bibliography of NBS publications concerning semiconductor measurement technology for the years 1962-1989] (March 1990).

This bibliography contains reports of work performed at the National Institute of Standards and Technology in the field of Semiconductor Measurement Technology in the period from 1962 through December 1989. An index by topic area and a list

Additional Information (cont'd.)

For authors are provided.

Contact: E. Jane Walters, (301) 975-050]

**NEW CALIBRATION SERVICES OFFERED**

The explosive growth of optical fiber use in the communications industry has resulted in a demand for calibration services. NIST's Boulder, Colorado, laboratory now offers measurements of optical laser power and energy at wavelengths and power levels of interest to fiber optic producers and users. Measurements are based on a standard reference instrument called the C-series calorimeter. An electrical-calibrated pyroelectric radiometer (CPR) is calibrated against the calorimeter and is then used to calibrate optical power meters at wavelengths of 850, 1000, and 1550 nm. To improve calibration capabilities, NIST is preparing test measurement systems for detector linearity, detector uniformity, and detector spectral responsivity. These systems could be available in 6 months. For a paper outlining NIST's optical power measurement capabilities, contact Fred Gehan, Div. 360, NIST, 325 Broadway, Boulder, Colorado 80303. For more information on calibration services, contact Thomas R. Scott, Div. 724, same address, phone (303) 497-3651.

**NEW NIST RESEARCH MATERIAL**

NIST has announced the availability of Research Material 8458, a well-characterized artificial flaw used as an artifact standard in eddy current non-destructive evaluation (NDE). The new Research Material (RM) is the outcome of work carried out by the Division to address the need for calibration standards for eddy-current NDE, for example as used to detect fatigue cracks in aircraft structures. The RM flaw is produced in annealed aluminum alloy block by first indenting the block and then compressive-deforming the resulting notch until it is tightly closed. The next operation is to restore a flat finish to the block

face, after which the block is heat treated to the original temper. The controlled flaw has been named the "CDF notch," after its inventors (listed on patent application) Thomas E. Capobianco (Electromagnetic Technology Division), William P. Dube (Division 583), and Ken Fizer (Naval Aviation Depot, NAS Norfolk, Virginia).

In the past, the challenge has been to manufacture artificial flaws that closely simulate the mechanical properties of fatigue cracks. Currently used artifacts include electrical-discharge-machined and saw-cut notches, both of which are relatively poor representations of fatigue cracks as their widths are too great. The Division-developed method provides notches that can be made controllably in a variety of geometries, with known dimensions, with widths that are narrow enough to provide an acceptable representation of fatigue cracks.

An NIST Research Material is not certified by NIST, but meets the International Standards Organization definition of "a material or substance one or more properties of which are sufficiently well established to be used in the calibration of an apparatus, the assessment of a measurement method, or for assigning values to materials." The documentation issued with RM 8458 is a "Report of Investigation." Contact: technical information -- Fred Fickett, (303) 497-3785; order information -- Office of Standard Reference Materials, (301) 975-6776.

**EMERGING TECHNOLOGIES IN ELECTRONICS...AND THEIR MEASUREMENT NEEDS, SECOND EDITION**

This report assesses the principal measurement needs that must be met to improve U.S. competitiveness in emerging technologies within several fields of electronics: semiconductors, superconductors, magnetics, optical fiber communications, optical fiber sensors, lasers, microwaves, video, and electromagnetic compatibility. The report seeks feedback from industry and Government

Additional Information (cont'd.)

agencies on the assessment. The feedback will guide the development of NIST programs that provide U.S. industry with new documented measurement methods, new national reference standards to assure the accuracy of those measurement methods, and new reference data for electronic materials. Copies may be obtained by ordering Report No. PB90-188087/AS (\$23.00 hard copy, \$11.00 microfiche) from the National Technical Information Service, 5285 Port Royal Road, Springfield, Virginia 22161, (703) 487-4650.

**JAN. 1, 1990 CHANGES IN THE U.S. ELECTRICAL UNITS**

Effective January 1, 1990, the U.S. as-maintained (i.e., "practical") units of voltage and resistance were increased by 9.264 ppm and 1.69 ppm, respectively. The increases in the U.S. legal units of current and of electrical power will be about 7.57 ppm and 16.84 ppm, respectively. These changes result from efforts by the major national standardizing laboratories, including the National Institute of Standards and Technology (NIST), formerly the National Bureau of Standards (NBS), to re-evaluate their as-maintained units in terms of the International System of Units (SI). The consequence of this activity has been the introduction of standards representing the SI units of voltage and resistance by the International Committee of Weights and Measures, an international body created by the Treaty of the Meter.<sup>1</sup> The use of these standards world-wide beginning January 1, 1990, will result in international consistency of electrical measurement as well as coherence among the practical units of length, mass,

electricity, time, etc., inherent in the definitions of the SI.

Implementation of Changes at NIST

These changes have been instituted in the U.S. by NIST using the new, internationally-adopted constants  $K_{J-90} = 483\,597.904\,619\,602\,328\,421\,015\,851\,966\,349\,045\,776\,000$  GHz/V exactly and  $R_{K-90} = 25\,812.807\,553\,380\,270\,709\,170\,224\,472\,660\,661\,361\,265\,836\,140\,64$  exactly with the Josephson and quantum Hall effects to establish representation of the SI volt and ohm, respectively. The representation of the SI volt is attained by using  $K_{J-90}$  in the formula

$$U_J(n) = \frac{f}{K_J} \quad n = 1, 2, 3, \dots$$

to give the voltages  $U_J(n)$  of the step produced by the ac Josephson effect at frequency  $f$ . The past value,  $K_{J-72}$ , was 483 593.42 GHz/V (NBS-72), thus leading to the 9.264 ppm change. Likewise,  $R_{K-90}$  is used in the following formula for the resistance of the  $i^{\text{th}}$  plateau of a quantum Hall effect device,

$$R_H(i) = \frac{R_K}{i} \quad (R_K = R_H(1))$$

to realize a representation of the ohm. The most recent past national unit of resistance,  $\Omega(\text{NBS-48})_t$ , was based on a group of five Thomas one-ohm standards and had an uncompensated drift rate of approximately -0.053 ppm per year. Since the quantum Hall effect is used as the national standard, the U.S. representation of the ohm has no drift. (The past unit of voltage,  $V(\text{NBS-72})$ , was based on the Josephson effect since 1972, and accordingly had a zero drift rate.)

Reassignments to Non-adjustable Standards

Since the U.S. practical volt and ohm units increased on January 1, 1990, the changes must be implemented in non-adjustable standards calibrated in terms of  $V(\text{NBS-72})$  and/or  $\Omega(\text{NBS-48})$  only by reducing the values assigned to them propo

<sup>1</sup>Note that the SI Units have not been redefined; rather, they have been realized more accurately and a quantum physics representation of the ohm has been introduced, thus leading to the changes in magnitude of the practical or as-maintained units.

Additional Information (cont'd.)

onally. The examples given below show how to do this for a standard cell and a standard resistor.

Simple Adjustments of Values of Standards

Standard cell:

"Old" emf 1.0180564 V(NBS-72)

Multiply "Old" emf by 0.999990736 to get emf in terms of the present volt representation  $1.01804697 \approx 1.0180470$  V

Standard resistor:

"Old" resistance value  
9999.976  $\Omega$ (NBS-48)<sub>01/01/90</sub>

Multiply "Old" resistance by 0.99999831 to get the resistance in terms of the present ohm representation  
 $9999.9591 \approx 9999.959$   $\Omega$

At the above, "Old" refers to the value of the standard which would have been in use on January 1, 1990, had the changes not been made; i.e., if a correction curve based on its past assigned values has been employed to obtain the current-used value for a standard, the above presents a downward shift of the curve starting January 1, 1990. For resistance, the slope of the curve also changed (slightly) since  $\Omega$ (NBS-48) has a drift rate and  $\Omega$ (NIST-90) does not.

Do not send your standards to NIST for calibration on January 1, 1990, unless they are normally due then. The changes are accurately known and corrections to existing standards may be applied.

Adjustment of Instrumentation

The assigned or calibrated value of a standard is merely a label giving the magnitude of the parameter embodied in

the standard. The actual emf or resistance of a standard did not change on January 1, 1990; only what it is called should have changed. In the same sense, meter readings are labels giving the magnitudes of the parameters being measured. Readings taken after January 1, 1990 using unadjusted meters will be too large in magnitude. Adjustments to meters must have the effect of reducing the amplitudes of readings for fixed emf's or resistances.

Adjustable voltage and current sources or adjustable resistors for which nominal output is desired, on the other hand, must have their outputs increased proportionally by the above amounts. DVM calibrators are probably the largest class of this type of instrument.

Guidelines

The National Conference of Standards Laboratories (NCSL) and NIST have formed NCSL *ad hoc* Committee 91.4, Changes in the Volt and Ohm to assist industry and government laboratories in coming into compliance with the changes. A major responsibility of the committee is the generation and publication of a set of guidelines which describes unambiguous methods for adjusting standards and instruments, or their values, and delineates other types of problems which may arise, e.g., voltage values called out explicitly in maintenance procedures, values imbedded in software, and the like. These guidelines have been published as NIST Technical Note 1263, "Guidelines for Implementing the New Representations of the Volt and Ohm Effective January 1, 1990." This document is available at no charge through the NIST Electricity Division. To receive a copy, contact Sharon Fromm at 301-975-4222.

For further information, contact Norman B. Belecki (301-975-4223), Ronald F. Dziuba (301-975-4239), Bruce F. Field (301-975-4230), or Barry N. Taylor (301-975-4220).

Additional Information (cont'd.)**U.S. REPRESENTATIONS OF ELECTRICAL POWER AND ENERGY**

Watt, Var, Volt-Ampere  
 Joule, Watthour, Varhour  
 Volt-Ampere-hour, and Q-hour

Background

By international agreement, starting on January 1, 1990, the U.S. put into place new representations of the volt and ohm based, respectively, on the Josephson and Quantum Hall effects and which are highly consistent with the International Systems of Units (SI). Implementation of the new volt and ohm representations in the U.S. required that on January 1, 1990, the value of the present national volt representation maintained by the National Institute of Standards and Technology (NIST, formerly the National Bureau of Standards) be increased by 9.264 parts per million (ppm) and that the value of the national ohm representation be increased by 1.69 ppm (1 ppm = 0.0001%). The resulting increase in the national representation of the ampere is 7.57 ppm. The resulting increase in the national representations of the electrical quantities of power, namely the watt, var, and volt-ampere, and the quantities of energy, namely the joule, watthour, varhour, volt-ampere-hour, and Q-hour is 16.84 ppm.

The adjustment for electrical power and energy is generally very small compared to revenue metering measurement uncertainties (typically greater than  $\pm 0.1\%$ ) and therefore are not likely to have a significant effect. Adjustments do not need to be applied in the above instances. However, for the highest accuracy calibrations of power and energy standards having uncertainties less than  $\pm 0.020\%$ , adjustments should be made. Accordingly, all Reports of Calibration and Reports of Test issued by NIST after January 1, 1990, reflect the appropriate changes.

For instruments calibrated prior to January 1, 1990, adjustments to the calibration values due to the change in the volt and ohm can be made without instrument recalibration. The adjustments are exact and, if properly applied, will not introduce any errors. Examples given below will illustrate proper procedures for applying the new adjustments.

Adjustments for Wattmeters, Varmeters, and Volt-Ampere Meters

Calibrations of wattmeters, varmeters and volt-ampere meters at NIST provide customers with corrections and uncertainties given in units of watts, vars or volt-amperes, as appropriate. Applying the appropriate adjustment due to the new representations of the volt and ohm for power measuring instruments (i.e. wattmeters for "real power" and varmeter for quadrature or imaginary power) requires minor calculations. First, it is necessary to assess the magnitude of the calibration uncertainty in percent and then decide if applying adjustments for the change in the volt and ohm are required. To determine the percentage uncertainty, simply divide the uncertainty in watts, vars, or volt-amperes by the product of the applied voltage and current times the power factor (the real power) and multiply that quantity by 100 as

$$U\% = [(U_w, U_v, \text{ or } U_{va}) / (V_a \times I_a \times PF)] \times 100,$$

where

$U\%$  is the uncertainty in percent,  
 $U_w$  is the calibration uncertainty in watts,  
 $U_v$  is the calibration uncertainty in vars,  
 $U_{va}$  is the calibration uncertainty in volt-amperes,  
 $V_a$  is the applied voltage in volts,  
 $I_a$  is the applied current in amperes,  
 and  
 PF is the power factor (including its sign).

For example, if the uncertainty is stated on a Report of Calibration as  $\pm 0.0$

Additional Information (cont'd.)

watts for the calibration of a wattmeter at an applied voltage of 120 V and an applied current of 5 A at unity power factor, then

$$\text{Percent Uncertainty} = U\% = [(\pm 0.060 \text{ W}) / (120 \text{ V} \times 5 \text{ A} \times 1)] \times 100 = \pm 0.010\%$$

If the percentage uncertainty, as calculated above, is less than  $\pm 0.020\%$ , (as it is in the above example), then it is recommended that an adjustment of 0.0017% (0.001684% rounded to four significant decimal places) due to the new representations of the volt and ohm be applied.

The second step is the calculation of how large the adjustment will be (in units of watts, vars, or volt-amperes, as appropriate), due to the reassignment of the volt and ohm. For the same example given above, if the calibration correction was given in a Report of Calibration as +0.052 watts, then the adjustment due to the change in the volt and ohm may be calculated by multiplying the product of the applied voltage and current times the power factor by 0.000017 (0.0017% expressed in proportional parts), as

$$\begin{aligned} \text{Adjustment} &= (V_a \times I_a \times \text{PF}) \times 0.000017 \\ \text{Adjustment} &= (120 \text{ V} \times 5 \text{ A} \times 1) \times 0.000017 = 0.010 \text{ watts.} \end{aligned}$$

The resulting product should be rounded to the same number of significant decimal places as the old calibration correction as given. This result is then subtracted from the old calibration correction, as in the following example:

$$\begin{aligned} \text{Old Calibration Correction} \\ \text{(prior to 1/1/90)} &= (+0.052 \text{ watts}) \\ \text{less } 0.000017 \times \text{Applied} \\ \text{Volt-amperes} \times \text{PF} &= \underline{-\{+0.010 \text{ watts}\}} \\ \text{New Calibration Correction} \\ \text{(after 1/1/90)} &= (+0.042 \text{ watts}) \end{aligned}$$

If the old calibration correction (prior to 1/1/90) at test conditions of 120 V, 5 A, and at a power factor of 0.5 lag,

happened to be a negative quantity, for example, -0.031 watts, then the old calibrations correction would be decreased (made more negative) by 0.0017% of the applied volt-ampere product times the power factor, as in the following example:

$$\begin{aligned} \text{Old Calibration Correction} \\ \text{(prior to 1/1/90)} &= (-0.031 \text{ watts}) \\ \text{less } 0.000017 \times \text{Applied} \\ \text{Volt-amperes} \times \text{PF} &= \underline{-\{+0.005 \text{ watts}\}} \\ \text{New Calibration Correction} \\ \text{(after 1/1/90)} &= (-0.036 \text{ watts}) \end{aligned}$$

The process of making the corresponding change for the varmeter corrections is identical to that shown above. For volt-ampere meters, the adjustment is made independent of the power factor (i.e., a value of PF = 1 may be used). However, most varmeter and volt-ampere meter calibrations have stated uncertainties greater than  $\pm 0.020\%$ , and hence, would not require an adjustment.

Adjustments for Joule, Watt-, Var-, Volt-Ampere- and Q-Hour Meters

Applying adjustments to electric energy measuring instruments (i.e., joule, watt-hour, varhour, volt-ampere-hour, and Q-hour meters) for changes in the representation of the volt and ohm, is more straightforward because the common calibration constant for energy metering is expressed as a "percentage registration." The amount the registration is to be adjusted can be subtracted directly as a percentage, regardless of power factor.

For example, if a watthour meter has a registration of 100.015% before January 1, 1990, then after that date, the new assigned registration would be decreased by 0.0017% (rounded from 0.001684%) as

$$\begin{aligned} \text{Old percentage registration} \\ \text{(prior to 1/1/90)} &= 100.015\% \\ \text{less amount due to change} \\ \text{in volt and ohm} &= \underline{-0.0017\%} \\ \text{New percentage registration} \\ \text{(after 1/1/90)} &= 100.0133\% \end{aligned}$$

Additional Information (cont'd.)

Rounded to three significant  
decimal places = 100.013%

The process of making the corresponding changes for the joule, varhour, volt-ampere-hour and Q-hour meters are identical to that shown above. If the associated uncertainty of the calibration is greater than  $\pm 0.020\%$ , no adjustments are necessary, as stated in the instances for wattmeters, varmeters, and volt-ampere meters. The uncertainties for varhour, volt-ampere-hour, and Q-hour meters are seldom less than  $\pm 0.020\%$ , and hence adjustments generally do not need to be made.

Reference

N. B. Belecki, R. F. Dziuba, B. F. Field, and B. N. Taylor, Guidelines for Implementing the New Representations of the Volt and Ohm Effective January 1, 1990, NIST Tech. Note 1263, June, 1989.

Copies of the above document are available at no cost from:

National Institute of Standards and  
Technology  
Electricity Division, MET B146  
Gaithersburg, MD 20899  
Telephone: (301) 975-4222

For Further Information

For further information concerning the above information, contact either John D. Ramboz (301) 975-2434 or Thomas L. Nelson (301) 975-2427, or write:

National Institute of Standards and  
Technology  
Electricity Division, MET B344  
Gaithersburg, MD 20899

**NEW BROCHURE FOR SEMICONDUCTOR SRMS**

Standard Reference Materials for Semiconductor Manufacturing Technology lists a series of SRMs for use in characterizing semiconductor materials and proces-

ses. The SRMs include a series of silicon resistivity materials for calibrating four-probe and eddy-current test equipment [Technical Contact: James R. Ehrstein, (301) 975-2060]; sizing materials for calibrating optical microscopes [Technical Contact: Robert D. Larrabee (301) 975-2298]; SRMs for optical measurements [Technical Contact: Jon Geist (301) 975-2066]; and sizing materials for calibrating scanning electron microscopes, SRMs for mechanical testing, X-ray and photographic films, X-ray diffraction, and the chemical analysis of materials [General Contact: Office of Standard Reference Materials, Cincinnati, Leonard, (301) 975-2023].

**1991 CEEE CALENDAR**

January 30-31, 1991 (New Orleans, LA)

**SEMATECH/ASTM/SEMI/NIST Workshop Silicon Materials for Mega-Applications.** To foster the understanding of circuit requirements and silicon properties that affect circuit performance, SEMATECH, ASTM, SEMI, and NIST are sponsoring this Workshop on mega-IC applications. Working sessions will consider requirement and specific issues on the following topics: silicon substrate and epi wafers, epitaxial processes, silicon on insulator technologies, contamination issues, and diagnostics and metrology. As this Workshop is being held in conjunction with meetings of SEMI Standards Committees and ASTM Committee F-1 on Electronics, a parallel aim of the Workshop is to provide guidance to and increased participation in the silicon-related standard work of ASTM and SEMI.

[Contact: Robert I. Scace, (301) 975-2220]

March 18-21, 1991 (Research Triangle Park, NC)

**First International Workshop on the Measurement and Characterization of Ultra-Shallow Doping Profiles in Semiconductors.** Sponsored by Microelectroni-

Additional Information (cont'd.)

Center of North Carolina (MCNC) in cooperation with the Semiconductor Research Corporation, the National Institute of Standards and Technology, and Northern Telecom Electronics, this workshop will provide a forum for a thorough discussion and evaluation of the different one- and two-dimensional techniques available for the measurement of ultra-shallow doping profiles in semiconductors. To be presented are invited papers by preeminent authors assessing the state of the art of different measurement techniques along with a prognosis for future extension of each technique. Topics to be covered by contributed papers include sputter depth profiling techniques, spreading resistance measurements, other electrical characterization techniques, and microscopy for junction profiling and interface characterization. Strategies for forming very shallow junctions will be featured in a plenary session.

Contact: James R. Ehrstein, (301) 975-0100

April 2-4, 1991 (NIST, Gaithersburg, MD)

**Workshop on Testing Strategies for Analog and Mixed-Signal Products.** This workshop is intended to teach a new approach for optimizing the tradeoffs associated with production testing of analog and mixed-signal devices. Examples of products that can benefit from this testing approach range from integrated circuit digital-to-analog and analog-to-digital data converters to programmable filters to multirange precision instruments. The workshop is intended for test engineers, automatic test equipment applications engineers, calibration laboratory managers, and others interested in improving the efficiency of testing analog and mixed-signal products. A small set of practical mathematical tools will be introduced, with an emphasis on implementation using commercial software rather than on mathematical development. Some familiarity with the concepts of linear algebra and elementary statistics would be useful, but is not a

requirement. The workshop will feature practical examples and hands-on training. [Contact: T. Michael Souders, (301) 975-2406]

September 8-11, 1991 (Research Triangle Park, NC)

**Third Workshop on Radiation-Induced and/or Process-Related Electrically Active Defects in Semiconductor-Insulator Systems.** This workshop is sponsored by the Microelectronics Center of North Carolina (MCNC), North Carolina State University, and the University of North Carolina at Charlotte, in cooperation with the Semiconductor Research Corporation, the IEEE Electron Devices Society, and the National Institute of Standards and Technology. Some areas of interest are: relationships between processing and electrically active defect densities, measurement methods, theoretical modeling of electrically active defects, process control of the sensitivity of insulators to ionizing radiation, removal of radiation damage, controlled radiation standard sources, and memory effects.

[Contact: Jeremiah R. Lowney, (301) 975-2048]

**IEEE SPONSORS**

National Institute of Standards and Technology

U.S. Air Force

Newark Air Force Station; Hanscom Field; Rome Air Development Center; Space & Missile Organization; U.S. Air Force Headquarters; Wright-Patterson Air Force Base

U.S. Army

AVRADCOM (Aviation); Dugway Proving Ground; Fort Belvoir; Fort Monmouth; Fort Huachuca; Harry Diamond Laboratory; Materials & Mechanics Research Center; Night Vision Laboratory; Picatinny Arsenal; Redstone Arsenal; Strategic Defense Command; The Pentagon

Department of Commerce

National Oceanic and Atmospheric Administration

CEEE Sponsors (cont'd.)

Department of Defense	Center/Crane; Office of Naval Research
Advanced Research Projects Agency;	Naval Ship Research Development Center
Defense Communication Agency;	Naval Air Systems Command; Naval Air
Defense Nuclear Agency; Combined	Engineering Center; Aviation Logistic
Army/Navy/Air Force (CCG)	Center/Patuxent; Naval Explosive
Department of Energy	Ordnance Disposal Tech. Center
Energy Systems Research; Fusion Energy;	National Science Foundation
Basic Energy Sciences; High Energy &	National Aeronautics and Space
Nuclear Physics	Administration
Department of Justice	Goddard Space Flight Center; Lewis
Law Enforcement Assistance	Research Center
Administration	Nuclear Regulatory Commission
U.S. Navy	Department of Transportation
David Taylor Research Center; Naval Sea	National Highway Traffic Safety
Systems Command; Weapons Support	Administration
	MIMIC Consortium
	Various Federal Government Agencies





1. PUBLICATION OR REPORT NUMBER NISTIR 4496
2. PERFORMING ORGANIZATION REPORT NUMBER
3. PUBLICATION DATE January 1991

# BIBLIOGRAPHIC DATA SHEET

ND SUBTITLE  
r for Electronics and Electrical Engineering Technical Progress Bulletin Covering  
r Programs, July to September 1990, with 1991 CEEE Events Calendar

R(S)  
Gonzalez, compiler

PERFORMING ORGANIZATION (IF JOINT OR OTHER THAN NIST, SEE INSTRUCTIONS)  
DEPARTMENT OF COMMERCE  
NATIONAL INSTITUTE OF STANDARDS AND TECHNOLOGY  
GAITHERSBURG, MD 20899

7. CONTRACT/GRANT NUMBER
8. TYPE OF REPORT AND PERIOD COVERED July-September 1990

PERFORMING ORGANIZATION NAME AND COMPLETE ADDRESS (STREET, CITY, STATE, ZIP)

REMARKS  
Technical information included in this document has been approved for publication  
separately.

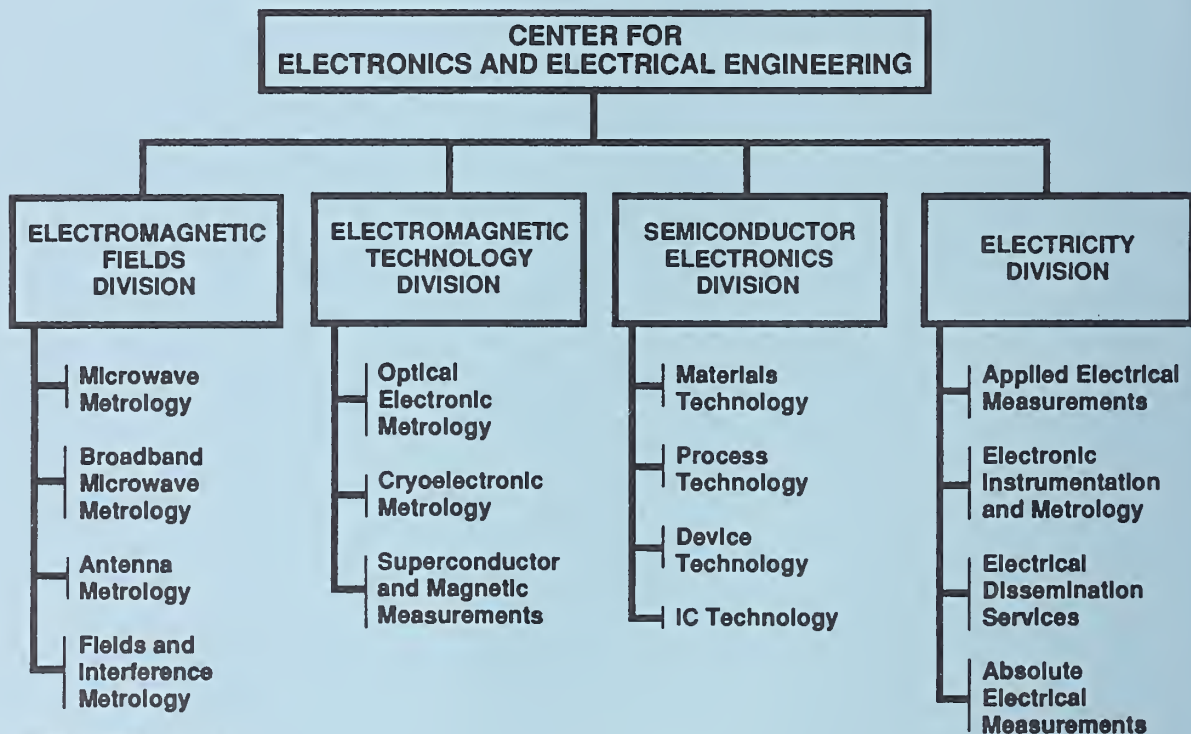
ABSTRACT (A 200-WORD OR LESS FACTUAL SUMMARY OF MOST SIGNIFICANT INFORMATION. IF DOCUMENT INCLUDES A SIGNIFICANT BIBLIOGRAPHY OR  
FUTURE SURVEY, MENTION IT HERE.)  
This is the thirty-second issue of a quarterly publication providing information on the  
technical work of the National Institute of Standards and Technology (formerly the  
National Bureau of Standards) Center for Electronics and Electrical Engineering. This  
issue of the CEEE Technical Progress Bulletin covers the third quarter of calendar year  
1990. Abstracts are provided by technical area for both published papers and papers  
submitted by NIST for publication.

KEYWORDS (6 TO 12 ENTRIES; ALPHABETICAL ORDER; CAPITALIZE ONLY PROPER NAMES; AND SEPARATE KEY WORDS BY SEMICOLONS)  
electronics; electrical engineering; electrical power; electromagnetic interference;  
electronics; instrumentation; laser; magnetics; microwave; optical fibers; semiconductors;  
conductors

AVAILABILITY  
UNLIMITED  
FOR OFFICIAL DISTRIBUTION. DO NOT RELEASE TO NATIONAL TECHNICAL INFORMATION SERVICE (NTIS).  
ORDER FROM SUPERINTENDENT OF DOCUMENTS, U.S. GOVERNMENT PRINTING OFFICE,  
WASHINGTON, DC 20402.  
ORDER FROM NATIONAL TECHNICAL INFORMATION SERVICE (NTIS), SPRINGFIELD, VA 22161.

14. NUMBER OF PRINTED PAGES 48
15. PRICE A03

OFFICIAL BUSINESS  
PENALTY FOR PRIVATE USE, \$300



NIST / CEEE / MAY 90

**KEY CONTACTS**

Center Headquarters (720)

Electromagnetic Fields Division (723)

Electromagnetic Technology Division (724)

Semiconductor Electronics Division (727)

Electricity Division (728)

Director, Mr. Judson C. French (301) 975-2220

Deputy Director, Mr. Robert I. Scace (301) 975-2220

Chief, Dr. Ramon C. Baird (303) 497-3131

Chief, Dr. Robert A. Kamper (303) 497-3535

Chief, Mr. Frank F. Oettinger (301) 975-2054

Chief, Dr. Oskars Petersons (301) 975-2400

**INFORMATION:**

For additional information on the Center for Electronics and Electrical Engineering, write or call:

Center for Electronics and Electrical Engineering  
National Institute of Standards and Technology  
Metrology Building, Room B-358  
Gaithersburg, MD 20899  
Telephone (301) 975-2220